A historical overview of steel tempering parameters

Lauralice C.F. Canale*

Departamento de Eng. Materiais, Aeronáutica e Automobilística
EESC – Universidade de São Paulo (USP)
Av Trabalhador São-carlense, 400
São Carlos, SP, CEP: 13566–590, Brazil
Fax: 5516 3373 9590
E-mail: lfcanale@sc.usp.br
*Corresponding author

Xin Yao

Department of Mechanical and Materials Engineering
Portland State University
P.O. Box 751
Portland, OR 97207–0751, USA
Fax: 503–725–8255
E-mail: tonyyao@cecs.pdx.edu

Jianfeng Gu

School of Materials Science and Engineering
Shanghai Jiao Tong University
800 Dongchuan Road, Shanghai 200240, China
Fax: +86–21–34203742
E-mail: gujf@sjtu.edu.cn

George E. Totten

Department of Mechanical and Materials Engineering
Portland State University
P.O. Box 751
Portland, OR 97207–0751, USA
Fax: 815–461–7344
E-mail: totten@cecs.pdx.edu

Abstract: The results of the stress relieving and tempering processes are dependent on the temperature and time of the process, which may be correlated using a parameter such as Holloman's (Holloman-Jaffe) parameter or the Larsen-Miller parameter. These parameters are a measure of the thermal effect of the process on the metallurgical transformation of the steel during tempering. The processes that exhibit the same tempering parameter are expected to exhibit the same effect (such as hardness). However, these more traditional numerical expressions assume isothermal tempering processes which seldom exist in production tempering ovens due to the heat-up period prior to soaking at the desired tempering temperature. Although the Larsen-Miller Equation and the Holloman-Jaffe parameter are well-known, their origin and limitations and, in some cases, their use, are often not discussed in detail in most heat treating texts. Therefore, a review of the metallurgy, origin, use and limitations of these expressions is provided here. In addition, recent work describing the development of more precise numerical relationships to describe the tempering process, including non-isothermal tempering processes, is also discussed.

Keywords: tempering; tempering parameters.

Reference to this paper should be made as follows: Canale, L.C.F., Yao, X., Gu, J. and Totten, G.E. (2008) 'A historical overview of steel tempering parameters', *Int. J. Microstructure and Materials Properties*, Vol. 3, Nos. 4–5, pp.474–525.

Biographical notes: Lauralice C.F. Canale is a Mechanical Engineer and received her MS and PhD degrees from Escola de Engenharia de São Carlos, Universidade de São Paulo (USP), Brazil. She has co-authored chapters and papers on heat treating, quenching, tribology and biomaterials. She is an Associate Professor at the same university (USP) and responsible for graduate and undergraduate courses.

Dr. Xin Yao has been a Postdoctoral Researcher at Portland State University in Portland, Oregon, USA, since he received his Doctoral degree from Shanghai Jiao Tong University, China. His research interests focus on the computer modelling of the thermal processing of metals and alloys, physical simulation and material thermophysical properties determination. He has about 20 publications.

Jianfeng Gu received his PhD from Shanghai Jiao Tong University, China. His main research interest is in numerical simulation on heat treatment process, such as quenching, nitriding, carburising, laser processing, *etc*., and he has over 40 published papers. Currently, He is an Associate Professor at the School of Materials Science and Engineering, Shanghai Jiao Tong University, Shanghai, China.

George E. Totten received his BS and MS degrees from Fairleigh Dickinson University in New Jersey and his PhD from New York University, USA. He has co-authored approximately 25 books and has approximately 500 patents and publications on various aspects of heat treating, quenching, hydraulic lubrication and tribology. He is the past President of the International Federation for Heat Treatment and Surface Engineering (IFHTSE). He is a Fellow of IFHTSE, ASTM, SAE and ASM International. Currently, he is a Research Professor at Portland State University, Portland, OR, USA.

1 Introduction

There are various methods of determining tempering time-temperature conditions. For example, one method that was reported by Liscic and Filetin (1987) used a two-step process to first compute the tempering temperature and then to compute tempering time at the required or 'optimal' temperature.

The first step of the Liscic-Filetin approach was to calculate the tempering temperature. The following equation which was developed by Just (1976) using multiple linear regression analysis and which was valid for tempering temperatures between 390°C–660°C was used to calculate the tempering temperature required to yield a design and alloy-specific hardness.

$$T_t = 917\sqrt[6]{\frac{\ln\left(\frac{H_q - 8}{H_t - 8}\right)}{S}} - 273°C \tag{1}$$

where:

T_t = absolute tempering temperature (K) – valid for $390 < T_t < 660°C$
H_q = hardness after quenching (HRC), which is calculated from: ($H_q = S(20 + 60 (C)^{0.5}$ HRC), where C = % carbon in the steel
H_t = required hardness after tempering (HRC)
S = grade of hardening which is calculated from: ($S = H_q$ measured / H_{max} possible), where H_{max} is the maximum possible as-quenched hardness for the steel grade being tempered.

The total tempering time including heat-up + soaking (holding) time is calculated from Jost's equation (Liscic and Filetin, 1987; Jost *et al.*, 1976):

$$t = a\frac{m}{A} + b \tag{2}$$

where:

t = time (min)
m = mass of the load or workpiece (kg)
A = total surface area (m^2) of the load or workpiece in contact with the heated furnace atmosphere
a and b = constants that are dependent on the mode of heating and specific equipment used and are determined by linear regression analysis of tempering time (t) and corresponding workpiece mass (m)/total surface area (A) for each furnace for which this equation will be used.

The value a will be the slope of this best-fit line and b will be the y-intercept and each furnace used for tempering.

The total soaking time depends on the design hardness value which is dependent on the mechanical requirements for the application. The total tempering time is also dependent on the size and shape of the load or workpiece being tempered using these relationships. It is assumed that cooling from the tempering temperature is in air. Faster cooling can be accommodated if appropriate computations are performed to account for the different heat transfer requirements (Liscic and Filetin, 1987).

Although useful for non-isothermal tempering processes in industrial furnaces, a disadvantage of this approach and other similar approaches is that there is a potentially wide array of time-temperature combinations that may be used to temper a steel alloy and also it is often inconvenient to perform such extensive experimental work to determine the necessary constants for every steel alloy and tempering condition that may be encountered. Therefore a major disadvantage is that the use of these does not permit interconversion of different tempering time and temperature combinations. Thus the need for a tempering parameter approach is established.

Tempering processes are dependent on both tempering temperature and time at temperature. Improper selection of these process parameters can potentially affect temper embrittlement, non-optimal stress relief, stress corrosion cracking, hardness, impact toughness, transformation of retained austenite and residual stress. Furthermore, appropriate temperature and time selection is dependent on carbon content and steel alloy chemistry. Figure 1 illustrates the interdependence of tempering temperature as a function of carbon content of a plain carbon (Fe-Fe_3C) steel (Krauss, 1980; Kern and Suess, 1979; Grange *et al.*, 1977).

Holloman and Jaffe developed a numerical relationship to predict the hardness of not only of carbon steels but also some alloy steels after tempering. This is the so-called Holloman-Jaffe equation (also generally known as the Larson-Miller equation) which is generally expressed by various authors as (Larson and Miller, 1952; Sinha, 2003; Hollomon and Jaffe, 1945; Pink, 1994; Manning, 1960; Mendelson *et al.*, 1965):

$$P_H = T_C(C + \log t) \times 10^{-3} \tag{3}$$

where:

P_H = the tempering parameter
t = the time (hours) at temperature T_C (in Kelvin)
C = the Holloman-Jaffe constant which is a material-dependent constant.

Typically, the most commonly reported forms of this equation use a value of C = 20. However, Grange and Baughman (1956), based on their work, recommended the value of C = 18 for all carbon and low alloy steels. It will be shown subsequently that the Holloman-Jaffe equation can be used to predict the as-tempered hardness for the tempering conditions shown in Figure 1.

These are useful computational methods to quantify tempering temperature and time for many steels and they have been used for many years (Kern and Suess, 1979). However, the actual historical development and metallurgical basis for these relationships and their limitations are much less well known. The first objective of this paper is to provide an historical perspective of the work leading to the development of these tempering equations.

The well-known Larson-Miller equation was developed to predict creep-rupture times although the equation is commonly used to predict tempering temperature-time cycles. Since this original work there have been a number of papers reporting various algorithms that have been developed to improve upon the Larson-Miller equation for the prediction of creep-rupture times. The second objective of this paper is to provide brief overviews of the potential use of two of these creep-rupture time equations; the relatively unknown Fullman parameter and the much more common Manson-Haferd equation, to predict temperatures and times.

Figure 1 Hardness of tempered martensite in iron-carbon (Fe-C) steel. These curves show the interrelationship of carbon content and hardness after tempering at various temperatures for one hour

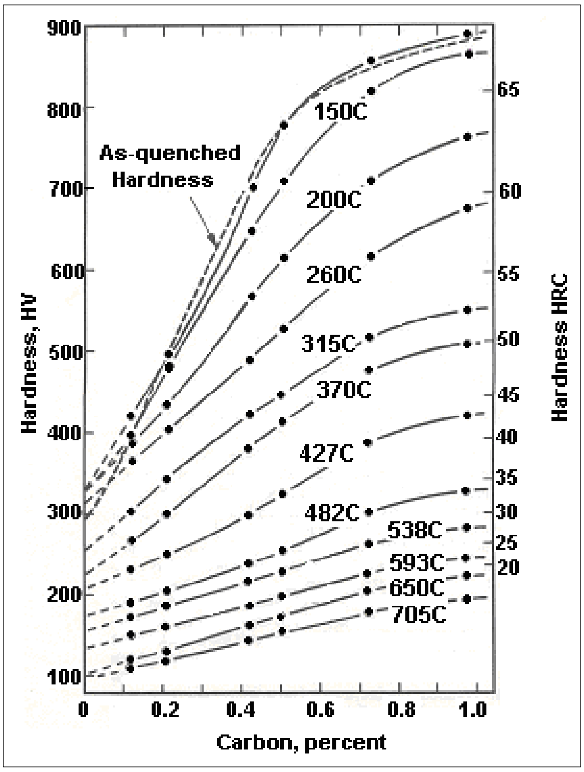

Source: Grange and Baughman (1956)

Recently, there have been various studies conducted to identify algorithms to compute tempering temperature-time relationships that provide greater accuracy for a broader range of steels and which address the impact of non-isothermal tempering cycles that include heat-up and cool-down processes that accompany industrial tempering processes and their potential impact on the desired metallurgical effect. The third objective of this paper is to provide an overview of and summarise the results of these studies.

2 Discussion

2.1 *Holloman-Jaffe equation*

In 1945, Holloman and Jaffe (1945) studied the effect of tempering temperature and time on the as-tempered hardness of six carbon steels with varying carbon contents ranging from 0.31%–1.51%. They assumed that hardness was an appropriately selected function of the diffusion equation (Holloman and Jaffe, 1945):

$$H = f\left[te^{-\frac{Q}{RT}}\right] \tag{4}$$

where:

H = hardness
t = the time at tempering temperature
T = the tempering temperature (absolute)
R = the ideal gas constant
Q = the activation energy for the structural changes involved in the tempering process of the steel
f = an appropriately selected function.

(It was also found that the value of Q was also dependent on hardness (Hollomon and Jaffe, 1945; Murphy and Woodhead, 1972)).

$$Q = f_2(H). \tag{5}$$

The assumption is that the tempering process can be explained using these relatively simple expressions and that for any particular hardness (Andrews, 1959), the structure change of the steel can be quantity will be a constant.

$$te^{-\frac{Q}{RT}} = t_o. \tag{6}$$

The value of Q can then be determined from the following logarithmic expression and by equating the relations for Q shown above:

$$Q = RT(\ln t - \ln t_o) = f_2(H). \tag{7}$$

Hardness can then be expressed by:

$$H = f_3[e^{RT\ln t/t_o}] = f\left(T\log {t}/{t_o}\right) = f[T\log t - \log t_o] = f[T(C + \log t)]. \tag{8}$$

When the hardness is constant, for example if equivalent tempering conditions (time and temperature) are considered to achieve a given hardness, and assuming the tempering temperature is constant during the process where the time (*t*) refers to the time at the tempering temperature, the interrelationship between Tempering Conditions (1) and Tempering Conditions (2) is given by (Hollomon and Jaffe, 1945):

$$T_1(C + \log t_1) = T_2(C + \log t_2). \tag{9}$$

Solving for the material constant C:

$$-C = \frac{T_1 \log t_1 - T_2 \log t_2}{T_1 - T_2} \tag{10}$$

$$\frac{T_1}{T_2} = \frac{C + \log t_1}{C + \log t_2} \tag{11}$$

$$C = -\log t_o \tag{12}$$

where t_o is dependent on the steel being tempered. These equations do not suggest anything regarding how hardness may vary with the tempering parameter but only that a relationship exists (Hollomon and Jaffe, 1945).

(Note: If the tempering temperature and time data for a tempering process, as determined from: log t versus 1/T, the slope of the line will be equal to: 0.434 Q/R. This is one method of determining values for Q.)

$$\log t - 0.434\left(Q/_{RT}\right). \tag{13}$$

The general equation: H = T (C + log t) is known as the Holloman-Jaffe equation. Holloman and Jaffe (1945) determined the value of C experimentally by plotting hardness versus tempering time for a series of tempering temperatures of interest and interpolating the data to obtain the time necessary to yield a number of different hardness values. This work was based on six different heats of plain carbon steels with carbon contents varying from 0.35%–1.15%. The time/temperature data pairs that yield the same hardness are then substituted into Equation (10) above to obtain the value for C. Also, from Equation (12), if the value of C is known, the value of t_o is easily determined.

It is interesting to note that the Holloman-Jaffe equation is a relatively strong function of temperature and a weak function of time (Andrews, 1959). Using this equation to fit their hardness and tempering time/temperature correlations, Holloman and Jaffe (1945) concluded:

- The data fit the equation to ± 1 HRC hardness units except when graphitisation occurred irregardless of the initial microstructure.
- The value of C varied somewhat for different steels and decreased linearly with the carbon content of a steel grade.
- The value of C was not critical in correlating the interdependence of tempering temperature and time.
- Holloman and Jaffe proposed that C = 19.5 for carbon and alloy steels with carbon contents of 0.25%–0.4%; C = 15 for tool steels with carbon contents of 0.9%–1.2%.
- If there is no secondary hardening, Rockwell and Brinell hardness varies almost linearly with C over a ‘considerable range’.

In Holloman and Jaffe’s work, the time was time at tempering temperature (isothermal), not the actual total time in the furnace (non-isothermal). However they reported that if desired, hardness corrections due to slow heating in the tempering furnace could be determined from (Holloman and Jaffe, 1945):

$$H = f_4 M \tag{14}$$

where M is the time-temperature correction parameter for cases when the temperature may vary – such as during heat-up in the furnace. The function f_4 was determined by Holloman and Jaffe from:

$$M = T\log(t/t_o) = \frac{T}{2.303\ln(t/t_o)} \tag{15}$$

$$t = t_o \times 10^{M/_T} \tag{16}$$

$$\frac{dM}{dT} = \frac{T}{(2.303t)} \tag{17}$$

by substitution of the value of t into the expression for dM/dt, the following equation is obtained:

$$dM = \frac{Tdt}{(2.303) \times 10^{(M/T)-C}} \tag{18}$$

where H = hardness, M is the time-temperature correction parameter that decreases as T increases during the heatup period to the isothermal tempering temperature and it is appropriate for boundary conditions for T log (t/t_o) and T (C + log t) expressions shown above. This equation is not only suitable for slow heating and cooling but also for processes where a tempered part is to a particular temperature where additional tempering may occur such as in a stress-relieving process (Holloman and Jaffe, 1945).

Holloman and Jaffe developed a series of nomograms for different carbon contents and total alloy contents for predicting tempering times. Their nomogram for predicting tempering times for steels containing 0.2%–0.4% carbon and low levels of total alloy content is shown in Figure 2 (Holloman and Jaffe, 1945). This nomogram is not applicable to steels that exhibit secondary hardening during tempering (Nehrenberg, 1950). The constant ‘C’ in the tempering equation was taken as 19,5 in the development of this nomogram.

Figure 2 Nomogram illustrating the interrelationship of tempering time, tempering temperature and the Holloman-Jaffe parameter (P)

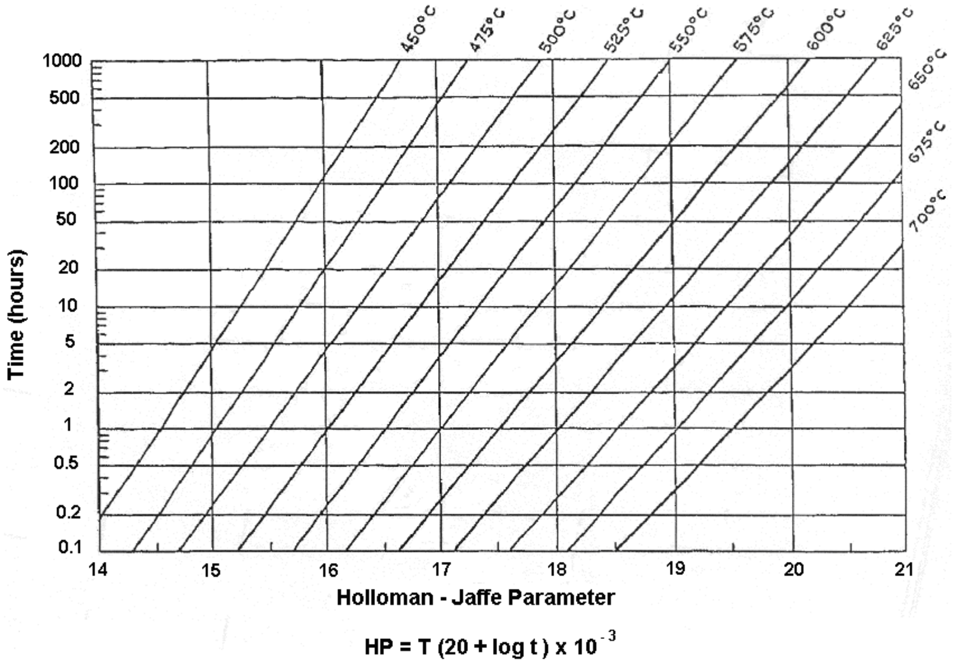

Source: Holloman and Jaffe (1945)

Waisman and Snyder developed a method of calculating total tempering time for multiple, and in some cases variable, temperature cycles by using a series of hardness versus tempering time for a variety of tempering temperatures (Waisman and Snyder, 1949). A good correlation was obtained for calculated versus experimental data as long as secondary hardening does not accompany tempering. The authors compared the results obtained by their experimental approach with those obtained by the Hollomon-Jaffe equation using the C-value of 20, and found generally good agreement as long as no secondary hardening occurs. However, they did show that dependable predictions cannot be made using the Holloman-Jaffe equation if there is no experimental tempering data available for validation of the predictions.

Empirical equations such as the Holloman-Jaffe equation can be very useful for tempering processes where sufficient data is available that adequately define the overall metallurgy of the steel being tempered. This is, in fact, a fundamental flaw of the use of any empirical relationships for which there is no metallography and hardness data available.

An example is provided by early work by Engel for a carbon steel with the following composition: C (0.94%); Mn (0.40%); Si (0.133%); P (0.034%) and S (0.44%) (Engel, 1939). In this work, steel test specimens were tempered at 315°C, 482°C, 565°C, 650°C and 704°C for times ranging from 2 sec to 22 h. It was shown that the degree of softening increased for all of the as-quenched microstructures (martensite, bainite and perlite) as the tempering temperature increased. However, the rate of softening for each structure was different from the others.

Furthermore, as the carbide size decreased, the rate of softening also decreased. In practice, this means if the section of steel did not harden throughout, a uniform hardness across the section can be achieved if appropriate tempering time is identified. Furthermore tempering beyond this point may result in the core being harder than the surface as illustrated in Figure 3 (Engel, 1939).

Grange and Baughman (1956) built upon the Holloman-Jaffe approach by experimentally determining the as-tempered hardness of various steel alloy compositions in order to examine the effects of elemental composition of the steel. The steels studied included 10XX and 40XX with varying carbon contents and also 2340, 5140, 6345 and 9264 steels. C-values were determined using the Holloman-Jaffe procedure described using the more extensive data available at the US Steel Laboratory. Their results showed that that the value of C varied from 15–20 (Grange and Baughman, 1956).

Grange and Baughman did report however, that the best fit of the equation through their data was obtained with a value of C = 18 and that the correlation was improved using DPH diamond pyramid hardness). DPH is now known as HV or Vickers hardness values. This variation was reportedly due to the greater penetration depth of measurement used to obtain Rockwell C hardness and resulted in less data scatter than achievable with the use of Rockwell hardness values. Therefore, DPH (Vickers hardness) was used for the work reported by Grange and Baughman (1956).

Grange and Baughman's work showed that alloying elements exhibited a resistance to softening during tempering, as observed from hardness measurements, and that the degree of this effect is dependent on the specific alloy present and its concentration. Also, this resistance to softening is independent of the carbon concentration in the 0.2%–0.85% range (Grange and Baughman, 1956).

Figure 3 Hardness distribution across a typical carbon steel cylinder (15/16 inch dia) containing 0.94% C with 0.4% manganese in the as-quenched condition and after three different tempering treatments described in the figure

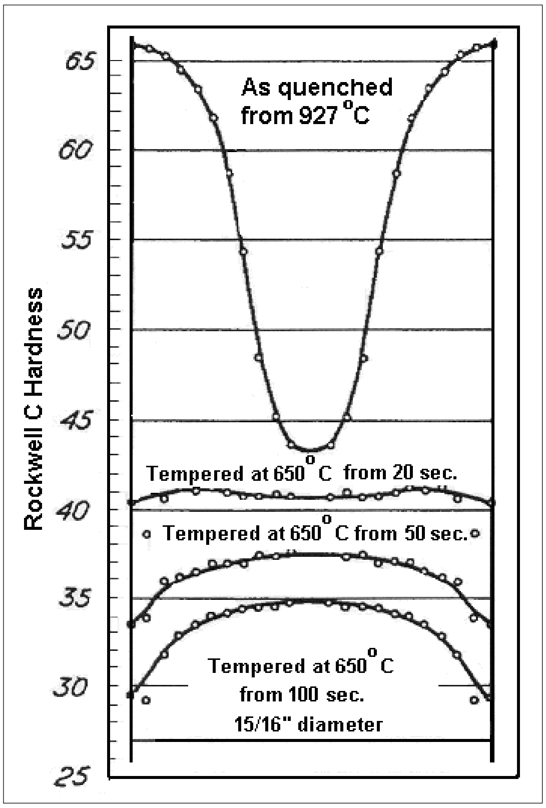

Source: Engel (1939)

Using the correction charts shown in Figure 2 (one chart for each tempering temperature), they developed a correction of hardness to the original Holloman-Jaffe equation based on the equation (Grange and Baughman, 1956):

$$\begin{aligned}\text{Estimated HV}(1000°F) = HV + \Delta HV_{Mn} + \Delta HV_P + \Delta HV_{Si} + \Delta HV_{Ni} \\ + \Delta HV_{Cr} + \Delta HV_V .\end{aligned} \quad (19)$$

These 'alloy factors' (expressed as HV increments) can be used to show the softening effect of the addition of different alloying elements to carbon steel by comparing the tempering curve and the corresponding carbon steel curve (Sinha, 2003). Grange and Baughman determined the incremental increase in hardness (resistance to softening) by measuring the Vickers hardness (DPH) of a steel with a known elemental composition at a series of different tempering parameters (temperature time variations) versus a plain carbon steel with the same carbon content (for example, see Figures 4a and 4b) (Grange *et al.*, 1977). These data are also summarised in Table 1 (Grange and Baughman, 1956).

Table 1 Correction factors (ΔHV_X) for predicting the hardness of tempered martensite

Element	*Range (%)*	*Factor at indicated tempering parameter value (ΔHV_X)*					
		20	*22*	*24*	*26*	*28*	*30*
Manganese	0.85–2.1	35	25	30	30	30	25
Silicon	0.3–2.2	65	60	30	30	30	30
Nickel	Up to 4	5	3	6	8	8	6
Chromium	Up to 1.2	50	55	55	55	55	55
Molybdenum	Up to 0.35	40 (20)[a]	90 (45)[a]	160 (80)[a]	220 (110)[a]	240 (120)[a]	210 (105)[a]
Vanadium[b]	Up to 0.2	0	30	85	150	210	150

Notes: [a] If 0.5-1.2 Cr is also present, use this factor.

[b] For AISI-SAE for chromium-vanadium steels; may not apply when vanadium is the only carbide former present.

Boron factor is 0.

Figure 4(a) and Figure 4(b) are tempering curves for AISI 4340 and 5140 steels respectively and a comparison of these curves confirm that different alloying elements affect the tempering behaviour of steel differently (Holloman and Jaffe, 1945). To more clearly observe the softening resistance effect of the alloying element in the alloy steel relative to an analogous carbon steel, the tempering curve for the corresponding carbon steel (AISI 1042) with the nominally the same carbon content is also shown on each figure.

Figure 4 (a) Grange and Baughman curve for AISI 4340 steel (b) Grange and Baughman curve for curve for AISI 5140 steel

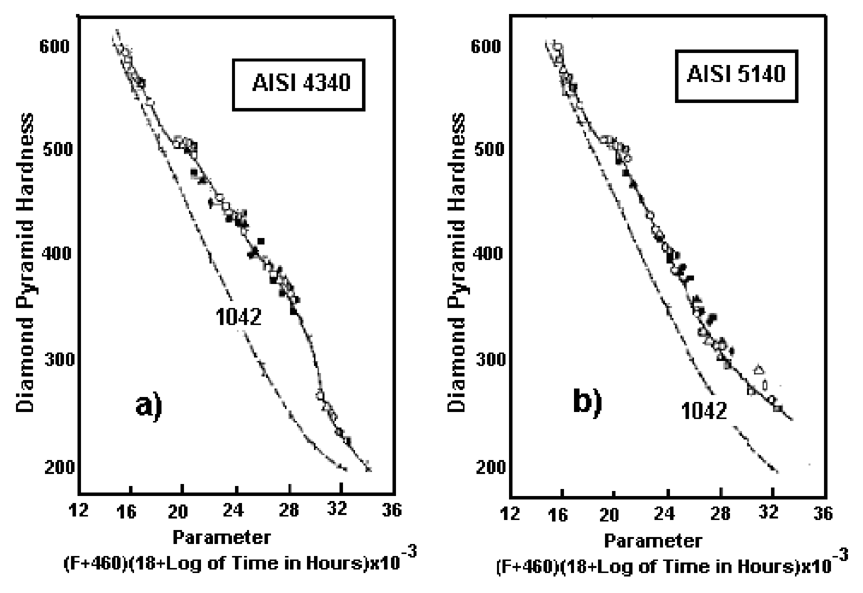

Source: Holloman and Jaffe (1945)

The following comments relative to these values were provided by Grange and Baughman (1956):

- Alloying elements exhibit their effect at different tempering temperatures when compared to other element.
- Since the effect of an alloying element is not directly proportional to the amount that may be present, relatively high concentrations may indicate an excessively high hardness when using Grange's alloy factors. Therefore, a concentration range for which the use of the given alloy factor is valid was provided.
- When two or more alloying elements are present, these elements tend to compete with each other as carbide formers and therefore the hardness calculated using the alloy factors may be greater than actually observed. This effect was addressed for Mo by decreasing its alloying factor by 1/2.
- At tempering temperatures lower than 343°C (650°F) (tempering parameter values less than 20), the resulting hardness of tempered martensite is influenced by rate of cooling during the prior quenching process and therefore by workpiece cross-section size and shape in addition to quench severity. This is due to the relative amount of retained austenite, particularly at lower carbon concentrations. This can also be affected by slower cooling through the martensite transformation range (M_s–M_f). The relative amount of *quench tempering* increases as the (M_s–M_f) temperature range increases. Therefore, due to potential unreliability, alloy factors below Tempering Parameter values of 20 are not provided.

Alloy factors are not included for tempering parameter values of 32 (and higher), because this corresponds to a tempering process of 1 h at 704°C (1300°F) which is greater than the Ac_1 temperature for nickel-containing steel. Although the Holloman-Jaffe equation can be used with reasonable success to estimate tempering time and temperature processes, the use of a single equation can lead to significant errors for most alloy steels. The approach provided by Grange and Baughman by the use of alloy factors, was shown to work well for a wide range of carbon and alloy steels if its use is restricted to 343°C–649°C (650°F–1200°F) and for a limited range of alloy concentrations.

Experimentally, families of curves showing the relative effects of different alloying elements on tempering behaviour were obtained by Grange *et al.* by tempering a steel test specimen of a plain carbon steel with a given tempering temperature and steel carbon content with a series of test specimens with the same carbon content but with increasing concentrations of the alloying element of interest. This work was repeated not only for varying alloying elements but for different tempering temperatures. From these families of curves, tempering curves showing the incremental effect on as-tempered hardness for varying alloying element concentration relative to a plain carbon steel, such as those shown in Figure 5 were constructed (Grange *et al.*, 1977).

The values of C used by Grange and Baughman were assumed, not experimentally derived. This was done to determine where the best data fit could be achieved. This was achieved at C = 18. Figure 6 shows that using a C-value of 18, a generally good fit of Vickers hardness for a range of carbon steels (AISI 1030, 1050 and 1080) with increasing carbon content is achievable (Grange and Baughman, 1956).

Figure 5 Effect of elements on the hardness of martensite tempered at different temperatures

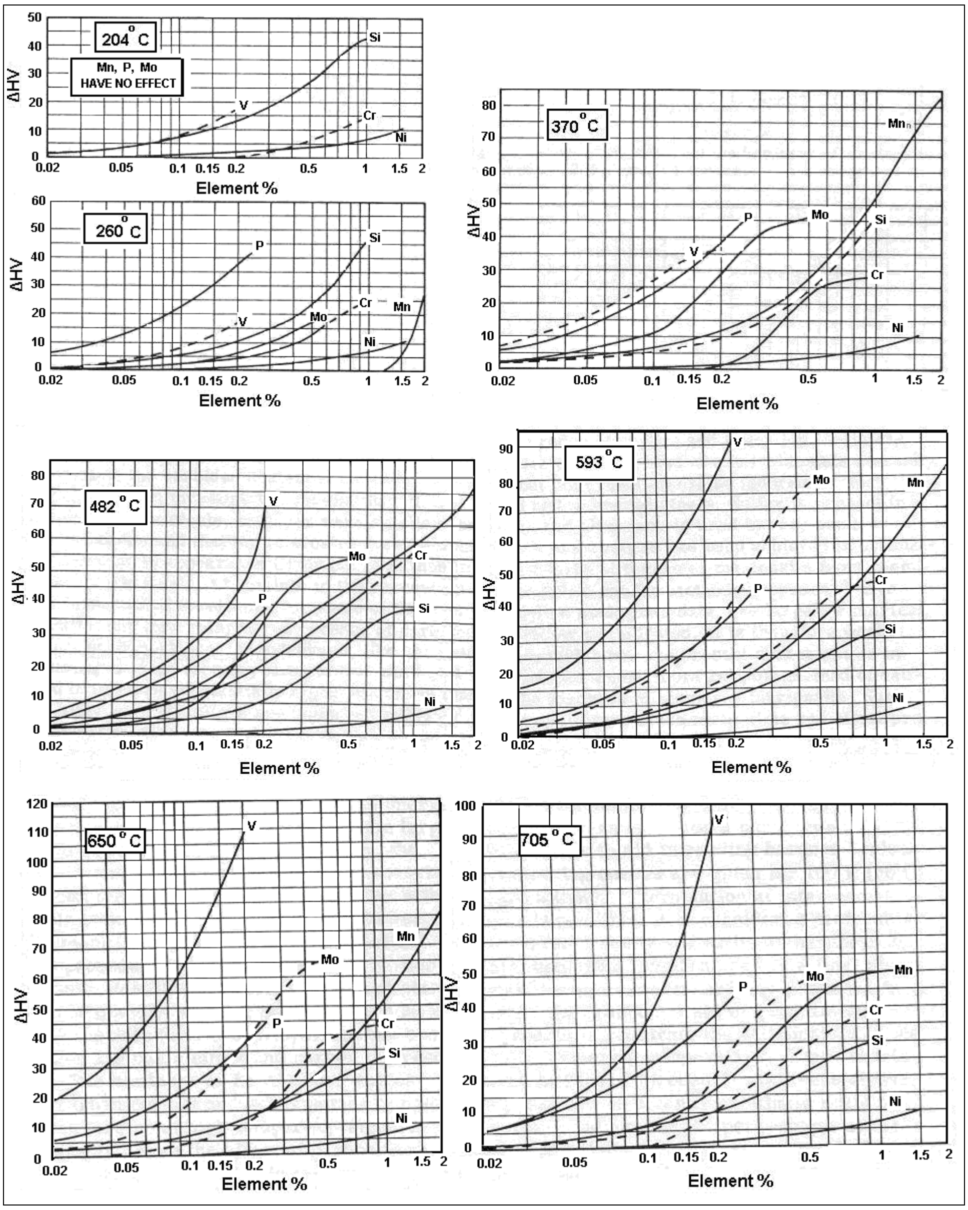

Source: Adapted from Grange *et al.* (1977)

Figure 6 Tempering parameter versus hardness curves for AISI 1030, 1050 and 1080 carbon steels. These data show good correlation for as-tempered hardness predicted by the tempering parameter when a constant C = 18 is used in the Holloman-Jaffe equation

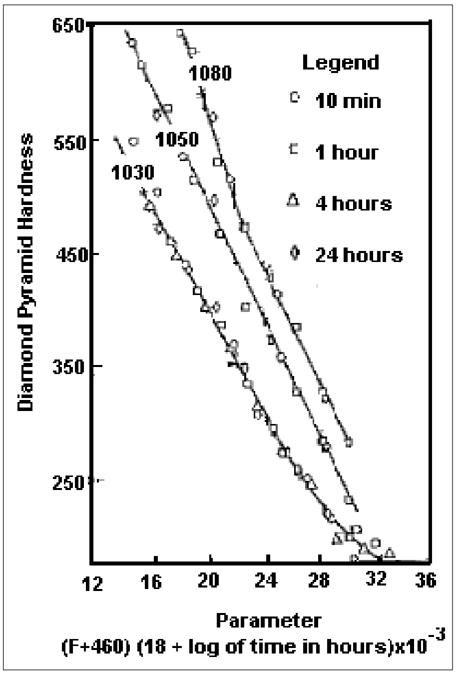

Source: Grange and Baughman (1956)

In addition to furnace tempering, where tempering times are typically measured in hours, the following form of the Holloman-Jaffe equation has also been successfully used for higher temperature, relatively short tempering times (seconds), such as for induction tempering (Anonymous, 1985a–b; Semiatin *et al.*, 1985b):

$$P = T(14.44 + \log t) \tag{20}$$

where T is absolute temperature in Rankine (°F + 460) and t is the induction tempering time in seconds. Holloman and Jaffe reported earlier that if one adds 3.57 to the C-value for tempering time in seconds (14.44), one obtains the C-value for tempering time in hours (Holloman and Jaffe, 1945). In this case, the equation would become P = T (18 + log t) which is the equation recommended by Grange and Baughman (1956).

There are two categories of induction tempering processes:

1 The first category of short time, high-temperature, rapid heating processes such as used for induction tempering, involve holding the steel for a fixed time (isothermal) and then cooling. Calculation of the tempering time using the Holloman-Jaffe equation is the same as that furnace tempering processes described previously.

2 The second category utilises tempering processes involving continuous heating and air cooling. The solution to this problem involves the derivation of an *effective tempering parameter* in order to correlate isothermal results such as those obtained by Category 1 processes (Pink, 1994; Anonymous, 1985b).

For processes involving continuous heating or cooling, Holloman and Jaffe suggested a numerical integration procedure. However, attempts to utilise this approach by Semiatin *et al.* (1985a) resulted in unacceptable computational instabilities. To resolve this problem, for induction tempering (a Category 2 process), the peak temperature is used for the temperature (T_{Peak}) and an effective tempering time (t_{eff}) is used for t in the Holloman-Jaffe equation (Semiatin *et al.*, 1985a). The value for T_{Peak} is assumed to be the temperature for the equivalent isothermal process. The process for determining t_{eff} is illustrated by the induction tempering cycle shown in Figure 7.

Figure 7(a) illustrates the heating and cooling portions of the induction tempering process where the cooling portion is somewhat slower than the heating portion of the process. For comparison, an equivalent isothermal process is illustrated in Figure 7(b). The solution to the problem of determining the value for (t_{eff}) is to segment the overall process into *i* time steps (Δt_i) which would have a temperature of T_i. However, Semiatin *et al.* assumed that $T_i = T_{Peak}$ = the maximum temperature of the process. The problem is then solved by summing the values for Δt_i shown in Figure 7(a) for the continuous cycle which is equivalent to the value for t_{eff}. Then the Semiatin *et al.* (1985a) equation for the Holloman-Jaffe parameter (P) for induction tempering processes is: $P = T_{Peak}$ $(C + \log t_{eff})$.

It is important to note that for induction tempering processes, there is critical temperature above which the temperature cannot be increased to accommodate reduced tempering times. This is called the *lower critical temperature* which is approximately 705°C for most carbon and low-alloy steels (Anonymous, 1985a–b).

Jarl *et al.* (2003) used the Holloman-Jaffe equation to determine equivalent tempering cycles in a molten lead bath relative to induction tempering by estimating tensile strength for a spring wire carbon steel (0.56% C). They found that although the variation in tensile strength was within ± 20 Mpa compared to experimental variation of ± 25 Mpa, the predicted tensile strength was consistently lower than the experimental value.

Figure 7 Schematic comparison of a continuous induction tempering cycle (a) with an equivalent isothermal tempering cycle (b) utilising an effective tempering time (t_{eff}) and temperature (T_{Peak}) as defined above

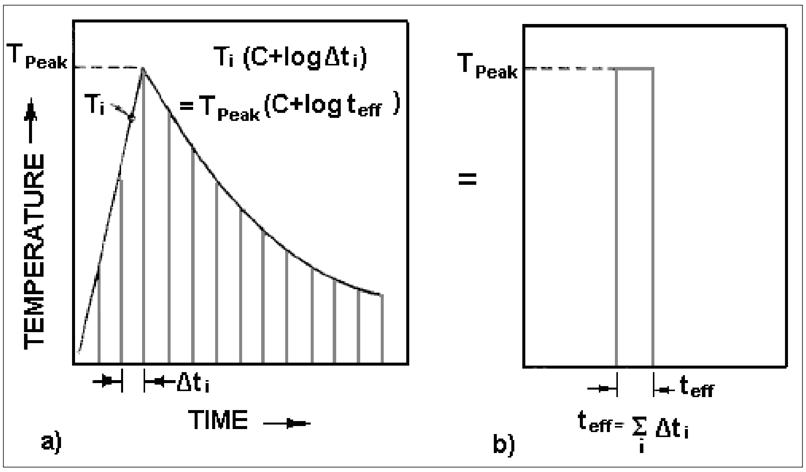

Source: Semiatin *et al.* (1985a)

The heat treatment process, especially tempering temperature and time, can significantly affect the resistance of construction steels to hydrogen embrittlement in a hydrogen sulphide media. Zikeev *et al.* (1984) studied the hydrogen resistance of a Russian steel (18Kh1G1MF = 0.19% C, 0.84% Mn, 0.29% Si, 1.27% Cr, 0.28% Mo, 0.06% V, 0.016% Al, 0.017% P, and 0.005% S; Ac_3 = 870°C).

One of the best methods of evaluating the effects of the entire range of tempering temperatures and time is to utilise the Holloman-Jaffe equation to correlate the property of interest with the tempering parameter. The equation for the Holloman-Jaffe parameter used by Zikeev *et al.* (1984) for their work was:

$$P = \frac{T(a + \ln t)}{1000} \tag{21}$$

where:

P = the Holloman-Jaffe parameter
T = the tempering temperature (K)
t = the tempering time (hr)
a = the Holloman-Jaffe constant.

For this work, Zikeev reportedly used an a-value of 40. The resistance of the steel to hydrogen embrittlement was determined by experimentally determining the tensile strength of unnotched 6 mm diameter samples in a deaerated saturated aqueous solution of hydrogen sulphide (pH = 2.9) up to a stress of $\sigma = 0.9$ and $\sigma_{0.2} = 500$ Mpa. In addition, the yield strength was also determined. Finally, the resistance of the steel to brittle fracture was determined from impact strength and the share of the ductile constituent in the fracture of the test specimens with a 1.0 mm notch radius at –100°C.

Figure 8 illustrates the linear correlation of the Holloman-Jaffe parameter of the 18Kh1G1MF steel with yield strength decreased with increasing values of the Holloman-Jaffe parameter (Zikeev *et al.*, 1984). Figure 9 illustrates the correlation of Holloman-Jaffe parameter to the brittle fracture of the steel (Zikeev *et al.*, 1984). Figure 10 illustrates the correlation of the Holloman-Jaffe parameter to resistance of the steel to hydrogen embrittlement (Zikeev *et al.*, 1984).

Figure 9 and Figure 10 show that there is a threshold character in the both the brittle fracture properties and the resistance to hydrogen embrittlement for the 18Kh1G1MF steel and that the observed transition in behaviour occurs for both properties for Holloman-Jaffe parameter values in the range of 33–38. Above the value of 38, a maximum level of brittle fracture and resistance to hydrogen embrittlement occurs. The similarity in Holloman-Jaffe tempering parameter performance with respect to both the brittle fracture and resistance to hydrogen embrittlement suggests an interrelationship between these two properties. Zikeev *et al.* (1984) proposed that this interrelationship was due to the hydrogen diffusion in the steel which in addition to temperature and loading rate leads to brittle fracture. Therefore, with knowledge of the Holloman-Jaffe parameter, it is possible to select the optimum tempering temperature and time conditions that will provide adequate strength and ductility properties of a construction steel while at the same time providing optimum resistance to hydrogen embrittlement.

Figure 8 Correlation of the Holloman-Jaffe parameter and yield strength for 18Kh1G1MF steel

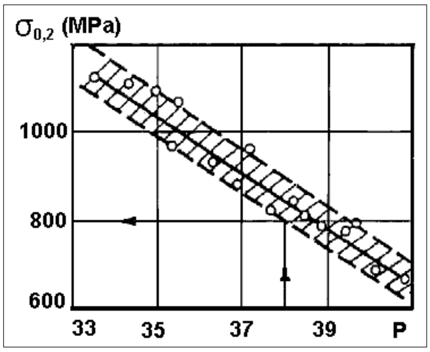

Source: Zikeev *et al.* (1984)

Figure 9 Correlation of the Holloman-Jaffe parameter and ductile fracture for 18Kh1G1MF steel

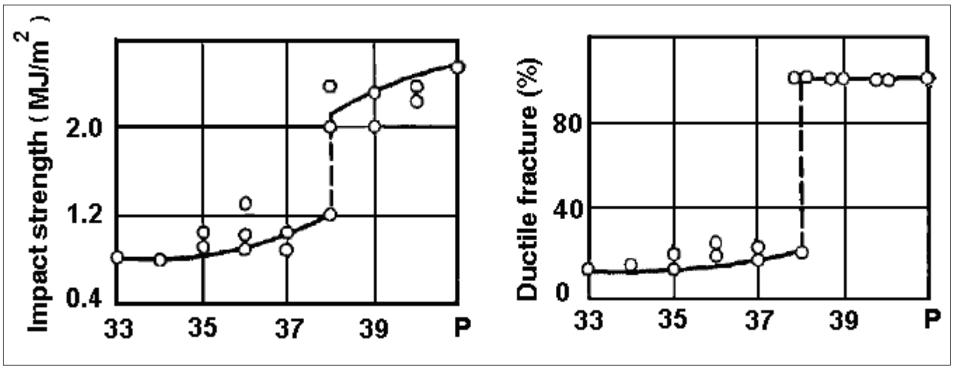

Source: Zikeev *et al.* (1984)

Figure 10 Correlation of hydrogen embrittlement of 18Kh1G1MF steel to the Holloman-Jaffe parameter

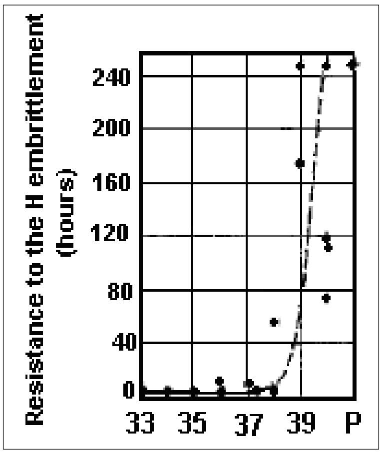

Source: Zikeev *et al.* (1984)

2.2 Nehrenberg master tempering curve

Nehrenberg (1950) developed a tempering curve based on previously published AISI 4340 Brinell hardness data (see Figure 11). From these data and earlier work of Holloman and Jaffe among others, Nehrenberg developed a tempering parameter (P) for the prediction of as-tempered hardness as a function of tempering temperature and time. It was reported that these data best fit the so-called Nehrenberg equation:

$$P = T(20 + \log t) \qquad (22)$$

where T is the absolute temperature and t is the tempering time in hours.

Figure 11 Nehrenberg master tempering curve for AISI 4340 which was derived from a 1 inch (25.4 mm) cross-section size of a steel bar that was tempered after oil quenching from 1500°F (816°C)

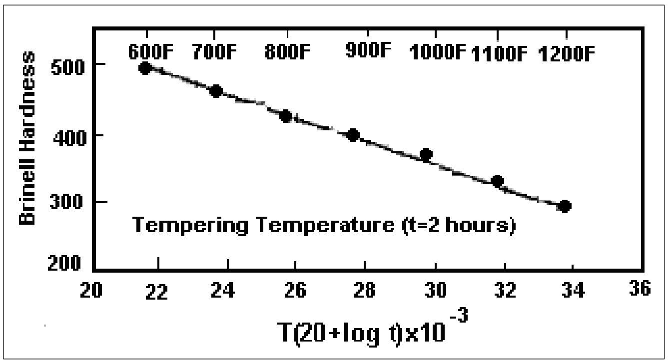

Source: Nehrenberg (1950)

This equation was developed based on Nehrenberg's tempering studies using hardenable stainless including Type 410, 416 and 420 stainless steel and a number of high-alloy, hot-work steels. Using the method described by Holloman and Jaffe for determination of the Holloman-Jaffe *C-constant*, Nehrenberg (1950) determined that C = 20, although not critical, best fit the data for the stainless steels and high-alloy steels of his study. It is interesting to note that although Holloman and Jaffe (1945) reported that the C-constant did vary for different steels, the value of 19.5 best fit their data for most carbon steels. The Nehrenberg equation is consistent with Holloman and Jaffe's observations but somewhat different from the C-constant of 18 recommended by Grange and Baughman (1956).

Nehrenberg reported that the tempering nomogram was also applicable for multiple tempering cycles if conducted at the same temperature since tempering times are additive. This can also be calculated from Equation (22). For example, if the steel is double-tempered and the temperature of each cycle is the same, the total tempering parameter is equivalent to the sum of the tempering parameters calculated for each step. Similarly, if a double-tempering process is conducted where the tempering temperature is different for each step, the tempering parameter is calculated for each step using the temperature and time that the steel is held at that step and then the two tempering parameters are simply added to determine the overall tempering effect of the double-tempering process. In other words, the tempering parameters are additive (Nehrenberg, 1950).

2.3 Larson-Miller equation

The time-dependent total strain (extension + initial gage length) which occurs in a material under a constant applied *creep stress* (constant load divided by the original cross-sectional area of the test specimen) is called *creep*. In a creep test, this is called *creep strain*. Creep strain which occurs at a diminishing rate is called *primary creep* and the creep strain which occurs at a minimum and nearly constant rate is called *secondary creep*. Creep which occurs at an accelerating rate is called *tertiary creep* (Davis, 1992). Steels may undergo embrittlement under creep conditions which is due to the presence of impurities such as, phosphorous, sulphur copper, arsenic, antimony and/or tin which will result in failure by intergranular cracking of the embrittled material (Davis, 1992).

A creep rupture test measures the extension of a metal under a given load and temperature until the test specimen ruptures. Creep strength is defined as the stress which will cause a given creep strain over a specified time and environmental condition and is obtained the time-elongation curves obtained at a constant load and the results are expressed as elongation (in millimetres or inches per hour for a given gage length, *e.g.*, 25 mm or 1 in Davis (1992). Laboratory creep tests are typically run between 100 and 10 000h, although creep acceptance tests may be run for shorter times and in some cases, creep rupture tests may be run for longer times. Most high-temperature materials are expected to last ten years or more, therefore, service stresses are typically lower than those used in the longest creep tests in order to generate data for most of the alloys used. To provide data for creep rates and rupture lives appropriate for establishing design stresses, it is of interest to be able to extrapolate creep performance from available data.

Larson and Miller reasoned that since various studies has shown that diffusion, tempering and creep processes seemed to follow the same rate process relationships then creep should also follow the previously reported Holloman-Jaffe relationship since it was derived from rate process theory. If creep could be described by the Holloman-Jaffe equation, then this could provide a relatively simple computational procedure to predict long-time processes from creep data obtained from short-time tests. To determine if long-time, high-temperature, creep and rupture performance can be adequately predicted from laboratory testing data, they evaluated the use of the Holloman-Jaffe equation to model creep and rupture data for the following materials (Larson and Miller, 1952): low-carbon steel, carbon-molybdenum steel, Cr-Mo-Ti-B steel, 16-8 stainless steel, 18-8-Mo stainless steel, S-500 forged alloy, Haynes Stellite No. 34 cast alloy, and titanium D-9 forged alloy.

The first step of this process was to develop master rupture curves using the following form of the Holloman-Jaffe equation:

$$LM = T(20 + \log t) \tag{23}$$

where T is the absolute temperature in Rankine (R) and t is the rupture time in hours. For creep predictions, LM is the Larson-Miller parameter.

(Note: It is of historical interest to note that this is the same form as the Nehrenberg equation described above. However, although the Nehrenberg equation was developed in 1950 from the Holloman-Jaffe equation (1945) to describe tempering processes and the Larson-Miller equation was developed to predict creep-rupture times also from the Holloman-Jaffe equation in 1952, this form of the equation is commonly referred to the Larson-Miller equation whether it is used for tempering or creep-rupture (or other property predictions) irregardless of the fact that it was developed later.)

Although the value of C = 20 is often assumed for the Larson-Miller equation, the actual value for C at a given creep stress (σ) can be calculated at two test temperatures (T_1 and T_2) and the log t for each value of T using Equation (10) above and using the value of the Larson-Miller parameter calculated from: LM = T (C + Log t) as illustrated in Figure 12 (Huang, 2003).

Figure 12 Graphical determination of the material parameter C from creep rupture data

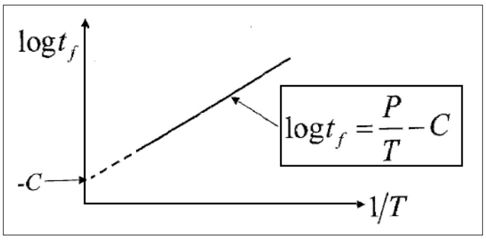

Source: Huang (2003)

Larson and Miller determined the value of C for different alloys and that data is summarised in Table 2. The span of the data was from C = 15 – 23 with an average of 19.3. Although they recognised that C may be material dependent, they reasoned that (Larson and Miller, 1952):

- The degree of data scatter was independent of the value of C.
- Since the variation of C was no greater in materials of widely different compositions relative to similar compositions, the differences may not be real.
- The use of a single value of C makes it possible to develop one single 'master curve'.

Table 2 Larsen-Miller C-value for different materials

Material	*C-value (for t in hours, T in R)*
Low-carbon steel	18
Carbon-moly steel	19
2 ¼ Cr and 1 Mo steel	23
Cr-Mo-Ti-B steel	22
18-8 stainless steel	18
18-8-Mo stainless steel	17
25-20 stainless steel	15
S-590 alloy	20
Haynes Stellite No. 34	20
Titanium D9	20

It is interesting to note that in the Discussion section of the now-classic Larson-Miller paper, J.J. Kanter used a speed-of-light calculation applied to a creep process and to independently calculated C = 18.39 – 18.43 for the materials studied by Larson and Miller (1952) suggesting that the value of C is essentially material independent. Using a

C-value of 18.43, Kanter derived the activation energies for the materials studied by Larson and Miller (1952) and Equation (2) (see Table 3) and he found that these values followed the commonly accepted order of high-temperature strength.

Table 3 Kanter's derived activation energies for materials studied by Larson-Miller

Material	*Q-value (cal / mole)*
Low-carbon steel	94 000
Carbon-moly steel	96 000
Cr-Mo-Ti – β-steel	100 000
18-8 stainless steel	112 000
18-8-Mo stainless steel	114 000
S-590 alloy	116 000
Haynes Stellite No. 34	116 000
Titanium D9	82 000

To eliminate the need for calculating the material constant (C) at different rupture times (t, hours) and test temperature (T, absolute) Larson and Miller (1952) developed the nomogram shown in Figure 13.

Figure 13 Larson-Miller test temperature versus the Larson-Miller (LM) parameter nomogram for various times (hours)

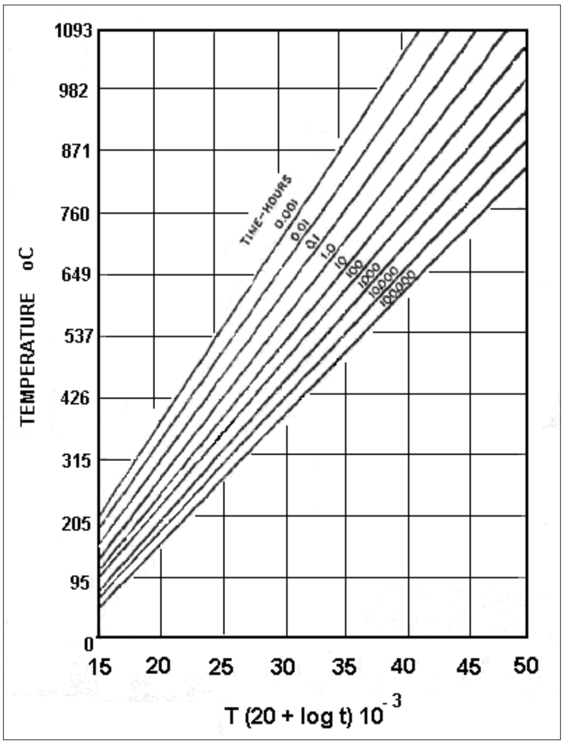

Source: Larson and Miller (1952)

Larson and Miller considered the effect of the magnitude of the error on the value of C (dC) selected. This error can be calculated from:

$$\frac{d(\log t_1)}{dC} = \frac{T_2 - T_1}{T_1}. \tag{24}$$

This equation shows that the error in the log t_l (log of tempering time) due to an error in the value of C is proportional to the difference in temperature ($T_2 - T_1$) and that this error would be expected to be relatively small except if the temperature difference is not large (Larson and Miller, 1952).

Brown *et al.* (1954) disagreed with Larson and Miller's assumption that the sensitivity of the prediction was independent of the value of 'C'. It was shown in earlier publications by Manson and Haferd (1953) and Manson and Brown (1952) that errors in prediction of creep and stress-rupture could vary significantly depending on the selection of the C-value for different materials. In fact, depending on the material, errors in predicted rupture time could be as great as an order of ten when using the Larson-Miller equation and C = 20. Furthermore, they found that, based on this earlier reported work (Manson and Haferd, 1953; Manson and Brown, 1952), the optimum value of 'C' could vary between 17–25, depending on the material and that the errors obtained for creep-rupture time was greater than the actual data scatter (Manson and Haferd, 1953; Manson and Brown, 1952). Finally, Brown *et al.* reported that the Manson-Haferd equation (see subsequent discussion) which utilises stress-independent material constants generally provided better data correlation than achievable with the Larson-Miller equation.

In a recent literature debate between Furillo *et al.* (1978) and DiMelfi (1978). Furillo *et al.* argued that the Larsen-Miller parameter was dependent on both temperature and stress and that the value of C, as determined from creep data, may vary between 8 to 57 depending on the steel alloy and thus should not always be assumed to be 20. Conversely, DiMelfi argued that the Larson-Miller equation, as it related to utility for creep predictions, was a function of stress only but that conclusion was contested by Furillo *et al.* From this debate, it is evident that whatever the correct position, when the Larson-Miller equation is used for creep calculations, care should be taken in the routine selection of C = 20, although it would seem to be adequate for tempering process parameter predictions.

A comparison of the master rupture curves obtained for the different alloys in this study are shown in Figure 13 (Larson and Miller, 1952). In addition to these eight curves, Larson and Miller (1952) applied this relationship successfully to over 40 alloys.

Larson and Miller also compared tempering and rupture data for a Cr-Mo-Ti-B steel. This comparison was of interest since both curves were obtained using the same equation and the results are shown in Figure 14 (Larson and Miller, 1952). The results obtained from this comparative study are shown in Figure 14. A sharp transition in rupture was observed which corresponded to the same point where a sharp transition in hardness was observed (Larson and Miller, 1952).

Figure 14 Larson-Miller master rupture curves correlating rupture strength with the for eight different alloys

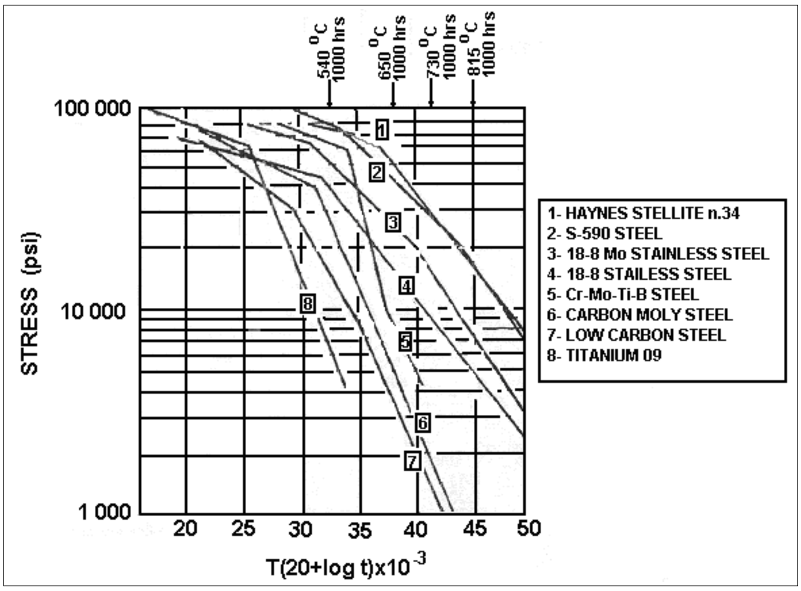

Source: Larson and Miller (1952)

Master creep curves can be constructed by one of two methods (Larson and Miller, 1952):

1 When the time to achieve a specific elongation is considered, the Larson-Miller parameter used is the same as that used for rupture analysis except that t is the time to achieve that amount of elongation.

2 If the minimum creep rate is considered, the Larson-Miller parameter calculation becomes:

$$Const = T(20 + \log r) \tag{25}$$

where r is the creep rate. The master creep curve for a carbon-molybdenum steel is shown in Figure 15 (Larson and Miller, 1952).

There are various reports describing the use of the Larson-Miller (Holloman-Jaffe) equation for assessing stress-relieving and tempering process conditions. Gingras and Grenier (2005) have developed a successful Excel-based graphical programme to estimate hardness afforded by different forced air tempering ovens, steel alloy, load size, *etc*.

Eriksson analysed the effect of heating and cooling (non-isothermal process conditions) during stress relieving on the use of the Larson-Miller equation (Gulvin *et al.*, 1972–1973). Based on this work, a modification of the Larson-Miller equation was reported for the calculation of *additional* 'equivalent' time (t_{eq}) at the tempering temperature for the heating and cooling portions of the overall tempering cycle (assuming that these are linear processes) (Gulvin *et al.*, 1972–1973; Ulff, 1970):

$$t_{eq} = \frac{T}{[2.3k(20 - \log k)]} \tag{26}$$

where T is the tempering temperature (K) and k is the heating or cooling rate in K/hr.

Figure 15 Comparison of the master rupture curve and tempering curve for Cr-Mo-Ti-B steel (T is in Rankine, r is the creep rate in %/h)

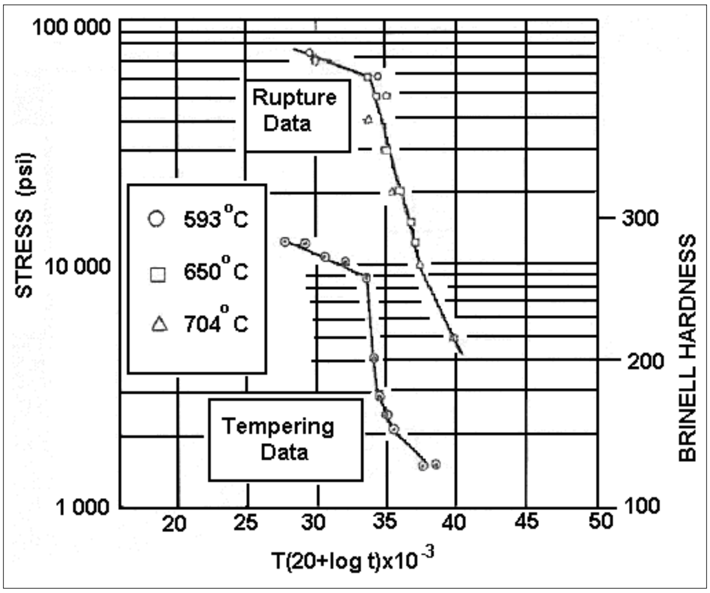

Source: Larson and Miller (1952)

The Larson-Miller equation has been used to estimate the effect of shorter times at higher temperatures on the tensile strength and ductility during ageing of dual phase steel wire (Dupla from Corus) used for fastener production (Trowsdale and Pritchard, 2006). The composition of this steel was: 0.08% carbon, 1.0% silicon, 1.7% manganese, 0.010% phosphorous, 0.005% sulphur, 0.016% chromium. Typical volume % of the microstructures exhibited by the as-rolled Dupla steel were: ferrite (70%–75%), pearlite (<2%), bainite (7%–13%), and martensite (15%–20%) and the ASTM grain size was 8–10.

Dual phase steels (*e.g.*, Dupla X60) achieve their strength through microstructure strengthening with an additional work hardening contribution. There was some concern that extended use at elevated temperature would result in a degradation of properties due to cold work recovery which would necessitate the establishment of an upper service temperature limit. Therefore, to determine if cold work recovery occurs under such conditions, a series of elevated temperature tests were conducted on drawn wire which was aged over a range of temperatures up to 400°C up to 1000 h. The Larson-Miller equation was used to interpret the results of these tests.

Figure 16 summarises the results of these tests. It was shown that increasing the aging temperature resulted in an increase in tensile strength. Thus, aging at 250°C for 1000 h was equivalent to 210°C for 100 000 h. In addition there was a corresponding increase in ductility as illustrated in Figure 16 (Trowsdale and Pritchard, 2006).

Figure 16 Effect of tensile strength and ductility variation on a dual phase spring wire (Dupla from Corus) after aging at an elevated temperature. For the equation above, the temperature is aging temperature in Kelvin and the aging time is in hours

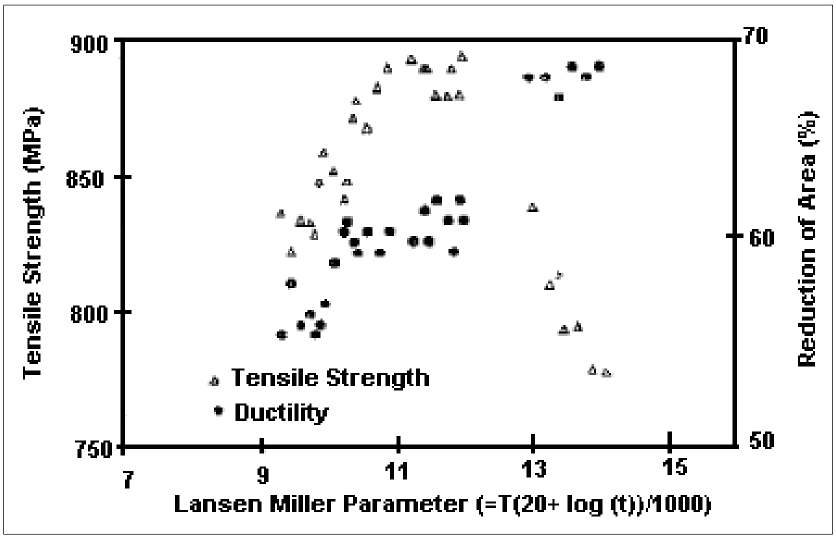

Source: Trowsdale and Pritchard (2006)

Welding processes are characterised by the presence of a Heat Affected Zone (HAZ). The HAZ in a weld is the area of base metal which has had its microstructure and properties altered by the heat from the welding process and subsequent re-cooling. The amount and magnitude of property change depends primarily on the base material, the weld filler metal, and the amount and concentration of heat input by the welding process.

For single-pass welds of C-Mn and low-carbon microalloyed steels, four characteristic microstructural zones may be identified: Coarse-grained HAZ (CGHAZ) which occurs from 1100°C to the melting point, Fine-grained HAZ (FGHAZ) which occurs from the Ac_3 temperature to 1100°C, Intercritical HAZ (ICHAZ) which occurs from the Ac_1 to the Ac_3 temperature, and the Subcritical HAZ (SC-HAZ) which occurs below the Ac_1 temperature. Since the CGHAZ region typically undergoes the most severe thermal process and since it usually exhibits the highest hardness, it is often of greatest interest (Ramierez *et al.*, 2005).

Post-weld heat treatment is performed welded steel to: improve mechanical properties, such as toughness, of a weld; to reduce high levels of residual stresses both across and along the weld caused by the welding process; and to decrease hardness within the weld to avoid the possibility of stress corrosion cracking (Ramierez *et al.*, 2005). The relative changes in these properties are due to metallurgical processes such as carbide formation due to the presence of vanadium or niobium which may induce strengthening from the distribution of finely divided carbides or carbonitrides. Vanadium and niobium carbonitrides are typically dissolved in austenite at the highest peak temperatures during welding and reprecipitate upon cooling. However, if these carbonitride particles do not precipitate on cooling, they may precipitate during subsequent subcritical thermal processes or during post-weld heat treatment. Since the solution temperatures of vanadium and niobium carbides are different, their precipitation behaviour would be expected to be different and therefore they would impact hardness (and other properties) during post-weld heat treating differently. This is why it is important to assess the effect of a particular microalloyed steel composition on post-weld heat treatment on a case-by-case basis (Ramierez *et al.*, 2005).

Ramierez *et al.* (2005) used of the Larson-Miller equation is to aid in the analysis of the HAZ to estimate the change in hardness of the CGHAZ of V-microalloyed X-60 steel due to tempering during post-weld heat treatment (635°C–670°C for 3–15 h). In this study, a single-pass welding process was simulated using a Gleeble. The CGHAZ thermal cycles with a peak temperature of 1320°C and cooling rates varying from 5°C/s–80°C/s through the temperature zone of 800°C–500°C were imposed on the V-microalloyed X60 steel pipe test specimen.

This study showed that post-weld heat treatment at 635°C with holding times between 3 and 15 h resulted in approximately parallel lines when the change in hardness between the initial hardness and as-tempered hardness versus the Larson-Miller parameter (Figures 17a and 17b) (Ramierez *et al.*, 2005). This data indicates that tempering effect, or change in hardness in the CGHAZ during the post-weld heat treatment, depends on the temperature and time of the process as indicated by the Larsen-Miller parameter correlation and also on the original hardness of the CGHAZ. The tempering effect due to the post-weld heat treatment increases with increasing as-welded hardness of the CGHAZ. This behaviour was possibly due to tempering of an increasing volume fraction of martensite/bainite in the CGHAZ as the as-welded hardness increased due to faster cooling a higher dislocation density and an increased potential for tempering. Interestingly, increased cooling rates would have been expected to lead to secondary hardening due to higher vanadium supersaturation of the CGHAZ. However, this was not observed since hardness changes during tempering due to secondary hardening from vanadium precipitates would have been expected to yield a non-linear response Figure 17(a) and 17(b). This example illustrates another potential use of the Larson-Miller (Holloman-Jaffe) equation to analyse tempering effects (Ramierez *et al.*, 2005).

Figure 17 (a) Effect of tempering on the change of CGHAZ hardness as of as-welded hardness and the Larson-Miller parameter. (b) Hardness of the CGHAZ as function of the as-welded function of as-welded hardness and the Larson-Miller parameter

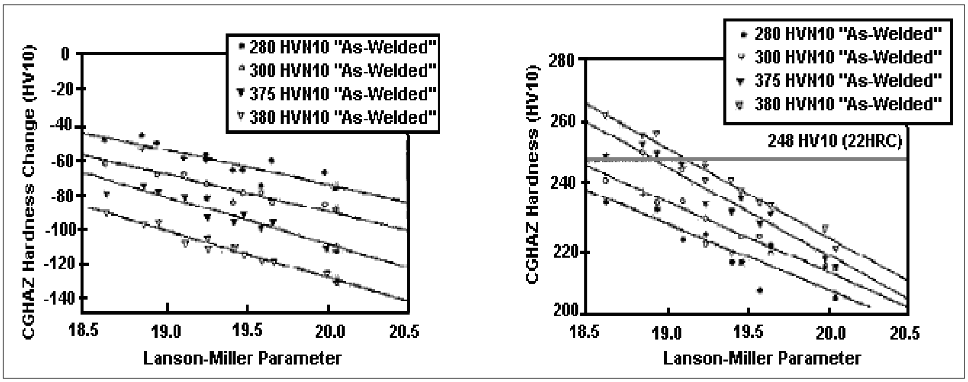

Source: Ramierez *et al.* (2005)

2.4 The Fullman parameter

Fullman disagreed with Holloman and Jaffe's assumption that the value of 'Q' in Equation (4) is variable and that 'A' is constant. In fact, as a number of reviewers have stated, Holloman and Jaffe's assumptions are neither typically accepted or theoretically justified (Murphy and Woodhead, 1972; Andrews, 1959). Fullman noted that transformation kinetics typically follow the form:

$$\frac{dU}{dt} = f_o(U)xe^{-Q/RT} \tag{27}$$

where:

Q = the activation energy
R = the gas constant
U = a fraction transformed
$f_o\,(U)$ = not constant but function of U.

For example, the rate of change of composition in one-dimensional diffusion assuming that the diffusivity is independent of composition at a particular position X would be:

$$r = \frac{\partial C}{\partial t} = D_o\left(\frac{\partial^2 C}{\partial X^2}\right)xe^{-Q/RT} \tag{28}$$

where:

C = the concentration
D_o and Q = constants
$\partial^2 C/\partial X^2$ = function of the concentration change that occurred already.

Furthermore, the equation used by Holloman-Jaffe was not theoretically justified but was only selected because it empirically fit their experimental data. Based on their experimental data, Holloman and Jaffe showed that their relationship requires that the value of Q not be a constant. Thus Fullman argued that it is incorrect to utilise an empirical relationship that cannot be experimentally justified, although no experimental data was provided to support this assertion.

Fullman (1954) developed a relationship based on Johnson and Mehl's geometrical relationships of heterogeneous transformations using standard kinetic theory which would provide a new time-temperature relationship based on the above kinetic relationship (Equation 29). If nucleation and growth have the same activation energy, Equation (29) can be rewritten as:

$$f_1U - f_1U_o = te^{-Q/RT} \tag{29}$$

and which can be rewritten in logarithmic form:

$$\log[f_1U - f_1U_o] = \log t - \left[\frac{Q}{(2.3RT)}\right] = \log t - bT. \tag{30}$$

The value log $[f_1U - f_1U_o]$ is a function of the extent of the transformation process. Another form of this equation is the so-called Fullman Parameter (FP) (Fullman, 1954):

$$FP = \left[\log t - \left(b/T \right)\right] \tag{31}$$

where:

t = tempering time (hr)
T = absolute tempering temperature (in Kelvin)
b = a constant reported to be equal to 15×10^3 (Fullman, 1954).

Murphy and Woodhead (1972) subsequently determined the value of b to be equal to 14.03×10^3 based on more extensive experimental data.

Murphy and Woodhead performed a study to compare the various published tempering parameters using an extensive data set of a carbon steel (0.39%) containing 0.71% Mn, 0,22& Si, 0.02% Cr and not more than 0.01% Ni, Mo, and V. One of the parameters that they studied in comparison to the Holloman-Jaffe parameter was the Fullman parameter. The ability of both the Fullman parameter and Holloman-Jaffe's equation to fit their steel tempering data and Woodhead and Murphy is shown in Figure 18(a) and 18(b) respectively. Based on analysis of these results, they concluded that both equations were essentially comparable for fitting steel tempering performance (Murphy and Woodhead, 1972).

Figure 18 Results of the Murphy and Woodhead comparison of the hardness correlation for tempering of a 0.39% carbon steel using the Fullman (a) and Holloman-Jaffe (b) tempering parameters

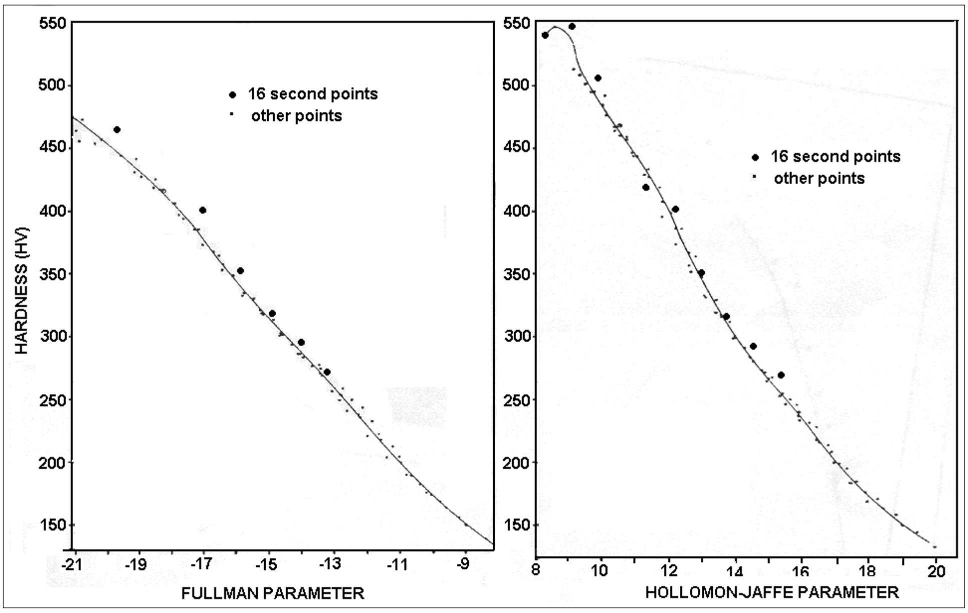

Source: Murphy and Woodhead (1972)

2.5 Manson-Haferd creep-rupture time parameter

Murphy and Woodhead (1972) also evaluated the use of the Manson-Haferd creep parameter (S) which was developed to analyse stress-rupture data for a variety of materials (Pink, 1994; Manning, 1960; Murphy and Woodhead, 1972; Manson and Haferd, 1953; Taylor and Johnson, 1971). The general form of the Manson-Haferd equation is (Anonymous, 1985b):

$$\frac{T - T_a}{\log t - \log t_a} = S \tag{32}$$

where:

T = creep rupture temperature (°F)
t = the creep rupture time (hours)
T_a and $\log t_a$ = material constants.

The Manson-Haferd constant (S) is the only term dependent on the rupture stress and each line in the plot represents points of constant rupture stress. This equation was shown to exhibit excellent projections of long-time rupture data from short time, 30–300 h, experimental test data. However, as Pink has noted, since the temperature in the Manson-Haferd equation is not in a reciprocal form, this parameter does not possess any fundamental physical significance and is simply an empirical relationship (Pink, 1994).

The Manson-Haferd parameter (S) expresses the approximate linearity of the function log t versus T when a material is subjected to a constant nominal stress which converges to a single point with the coordinates of T_a, log t_a. Manson and Haferd reported that for the 40 materials that they studied, the use of stress-rupture data in the time range of <300 h yielded excellent correlation to the actual stress-rupture value obtained over longer times, up to 10 000 h. They did not recommend, however, the use of stress-rupture data obtained at <10 h because of the non-linearity of the extrapolation (Manson and Haferd, 1953).

The material constants T_a and log t_a may be extrapolated from rupture data such as that shown in Figure 19 (Manson and Haferd, 1953). These coordinates were not reported to have any physical significance and that they only represented a point of convergence of the tangents of the curve log t versus T. Manson and Haferd reported that typically, convergence occurs at a stress level which is approximately equal to room temperature ultimate tensile strength of the material.

Although the Manson-Haferd equation is reported to be preferable to the Larson-Miller equation to model creep-rupture at moderately high temperatures and at low stresses, it suffers from two further limitations:

1. since steady state creep is assumed to be the only mode contributing to deformation, primary and tertiary creep is not included
2. since the creep process is assumed to be steady-sate, possible changes in material structure are not considered (Pink, 1994).

Figure 19 Schematic diagram illustrating typical constant-time cross-plot used in the analysis of stress-rupture data using the Manson-Haferd equation

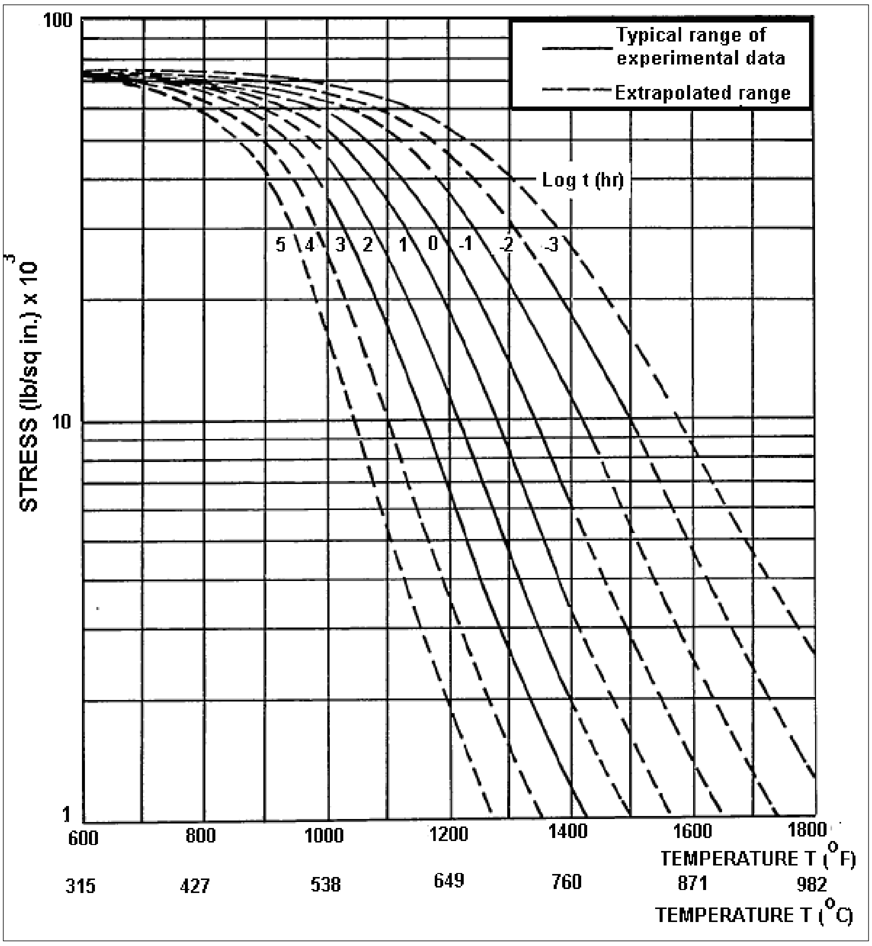

Source: Manson and Haferd (1953)

The following variation of the Manson-Haferd equation can be used to extrapolate total creep elongation rate (r) (Manson and Haferd, 1953):

$$r = \frac{T - T_a}{\log r + \log r_a} \tag{33}$$

where *r* is the minimum creep elongation rate and *log* r_a is a material constant.

Since the Larson-Miller equation was developed for use in analysis of creep data and since it is also commonly used to analyse tempering processes (as described previously), Murphy and Woodhead included evaluated fit of the of their tempering data for a carbon steel using a form of the Manson-Haferd equation. For this work, they used the values of 350 K and 14.1 for T_a and log t_a respectively. Figure 20 shows the correlation results of plotting log (t – 14.1) / (T-350) versus hardness (Murphy and Woodhead, 1972). The inverse form of the Manson-Haferd equation was plotted so that the data would be in a form similar to that used for the Holloman-Jaffe equation and the equation for the Fullman Parameter.

Figure 20 Woodhead and Murphy correlation of as-tempered hardness of a carbon steel as a function of the reciprocal of the Manson-Haferd parameter. The reciprocal of the Manson-Haferd parameter was used so that the curve fitting would be of the same form as that used for converting the hardness data to the Fullman parameter shown in Figure 18(a) and the Holloman-Jaffe parameter shown in Figure 18(b)

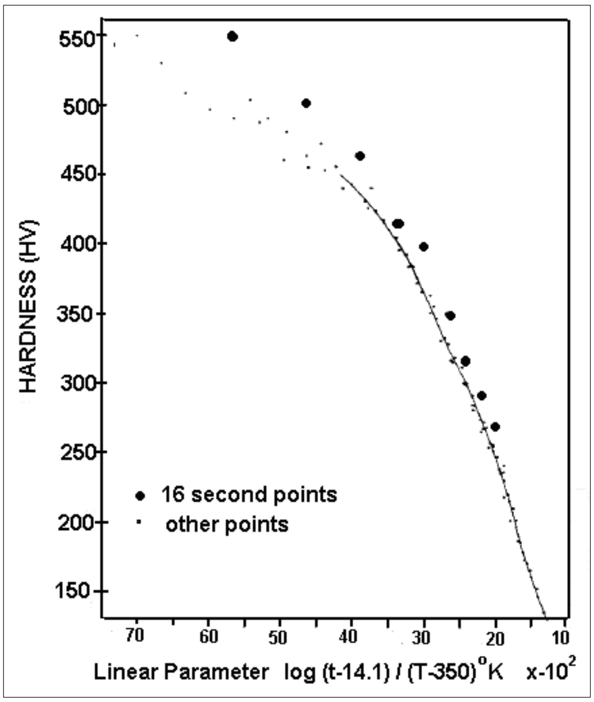

Source: Engel (1939)

The Murphy and Woodhead results showed that small changes in the Manson-Haferd parameter resulted in large variation of hardness. The results also are not satisfactory for short tempering times. Although the results obtained did not fit well for the early stages of tempering, a relatively good fit was obtained as the tempering process proceeds. This is noteworthy because the steepness of the curve implies that relatively small changes in the inverse of the Manson-Haferd parameter result in large changes in hardness (Murphy and Woodhead, 1972).

2.6 Mathematical model of Holloman parameter

Wan *et al.* (2005) developed a mathematical model based on Holloman's equation which provides a correlation for as-tempered hardness for various tempering times based experimental data for steels (that do not exhibit a secondary hardness effect) that were tempered for one hour at various tempering temperatures using the equation:

$$H_1 + T\left(\frac{dH_1}{dT}\right)\ln\left(1+\frac{\log\tau}{C}\right) \tag{34}$$

where:

H_1 = as-tempered hardness of the desired as-quenched steel alloy after tempering for one (1) hour at a given temperature (K)
T = the absolute temperature in Kelvin
τ = the tempering time in hours
$(dH_1/dT)_t$ = the change in hardness (HRC) with respect to temperature (K) (isothermal)
C = assumed to be 20 (as reported by Nehrenberg (1950) and Larson and Miller (1952)).

Wan *et al.* (2005) based their calculations on experimental Rockwell C Hardness (HRC) and derived the following regression equation for H_1 = HRC:

$$HRC = 13.88 + 40.36\exp[-6.1584\times10^{-10}(T-273)^{3.259}]. \tag{35}$$

A series of one-hour tempering curves for 42CrMo steel shown in Figure 21 (Wan *et al.*, 2005) were derived based on earlier work by Guo (1999).

Figure 21 Comparison of experimental and predicted one hour tempering curves obtained for 42CrMo steel after tempering at various temperatures

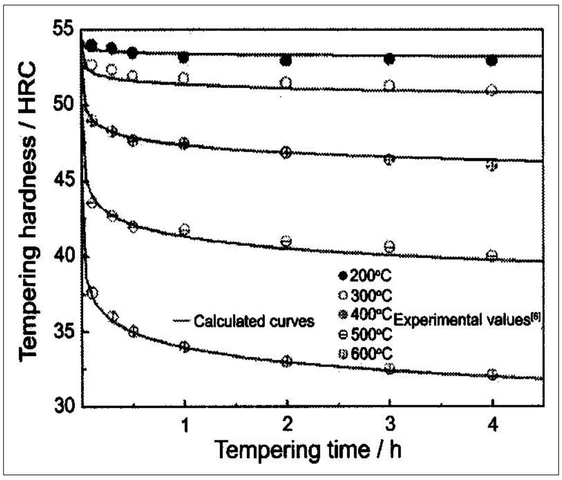

Source: Guo (1999)

Wan used these data to determine the tempering time (t) at a given temperature using the one-hour as-tempered data for 42CrMo steel and the following general equation (Wan *et al.*, 2005), derived from Equation (33) (derivation not shown here):

$$H = a + b\log t \tag{36}$$

where $a = H_1$ (HRC) which is material-specific and is essentially the hardness of a specific quenched steel tempered isothermally for one hour and b is defined for the same specific alloy of interest assuming no secondary hardening effects as (Wan *et al.*, 2005):

$$b = \frac{T}{C}\left(\frac{dH_1}{dT}\right) \tag{37}$$

where:

T = temperature (K)
C = assumed to be equal to 20
(dH_1/dT) = change in hardness with respect to temperature (isothermal) for a specific steel.

2.7 Time-temperature tempering kinetic law

Zhang and coworkers also studied the microstructural evolution during the tempering process of: 55NiCrMoV7 (AISI L6) (Zhang *et al.*, 2004). The objective of this work was to develop a kinetic law that would describe the softening of this steel during tempering. As a result of their experimental investigation where test specimens were austenitised for one hour at 875°C and then quenched in oil followed by isothermal tempering. As a result of this work, the experimental data shown in Figure 22 was obtained (Zhang *et al.*, 2004).

Figure 22 Hardness evolution during tempering of 55NiCrMoV7 (AISI L6) steel for temperatures between 100°C and 700°C

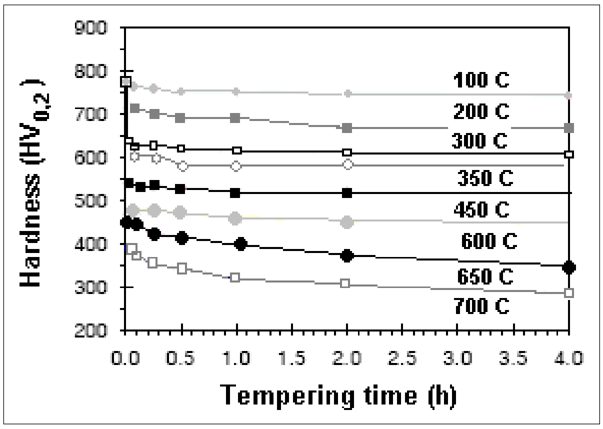

Source: Zhang *et al.* (2004)

The tempering process can be considered to be a phase transformation process which is dependent on diffusion from martensite (unstable state) to a state referred to by Zhang as a 'quasi-stable state' which is a mixture of ferrite and globular carbides. However, the difficulty is that hardness values for a particular material does not refer to a single state but any mixture that produces that same hardness. Since a single hardness value, by itself, does not indicate either softening from an as-quenched phase or hardening from an equilibrium state, the use of a tempering ratio (ι_V) is necessary (Zhang *et al.*, 2004):

$$\tau_V = \frac{H_V - H_o}{H_\infty - H_o} \tag{38}$$

where:

H_o = as-quenched hardness
H_∞ = hardness in a completely annealed state
H_V = hardness of a state intermediate between the as-quenched (H_o) and the completely annealed state (H_∞).

The tempering ratio will vary between '0' (as-quenched state and '1' (annealed state). Figure 23 illustrates tempering ratio values obtained for the 55NiCrMoV7 (AISI L6) steel that were experimentally obtained where: $H_O = 776(HV_{0.2})$ and $H_\infty = 210(HV_{0.2})$ (Zhang *et al.*, 2004). The tempering ratio increases exponentially with respect to time at tempering temperature the tempering ratio increases with temperature for the same tempering time.

Figure 23 Illustration of the experimentally measured tempering ratio with respect to tempering temperature and time for 55NiCrMoV7 (AISI L6) steel alloy

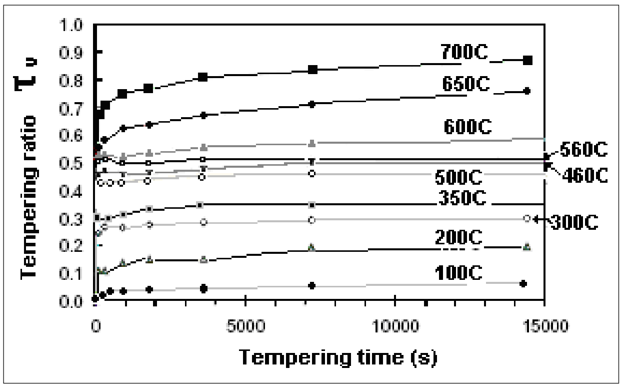

Source: Zhang *et al.* (2004)

The Johnson-Mehl-Avrami equation (Johnson and Mehl, 1939; Avrami, 1939; 1940; 1941) describes solid phase transformation controlled by diffusion and the equation for a tempering process where there is an evolution with respect to temperature and time of different mechanisms (carbide precipitation and growth) (DiMelfi, 1978). The Johnson-Mehl-Avrami equation can be used to model the transformation kinetics of a tempering diffusion process (Johnson and Mehl, 1939; Avrami, 1939; 1940; 1941):

$$\tau_U = 1 - Exp[-(Dt)^m] \tag{39}$$

where:

t = tempering time
m = material-dependent ageing exponent
D = diffusion rate which is dependent on tempering temperature (T) and follows the Arrhenius equation:

$$D = D_o Exp\left[{}^{-Q}\!/_{RT}\right] \tag{40}$$

where:

D_o = pre-exponential constant
Q = activation energy for tempering transformation (a typical value for low to medium alloy steel is approximately 2341 kJ mole^{-1}
R = ideal gas constant (8.31 JK^{-1}mole^{-1})
T = tempering temperature (K).

Equations (39) and (40) assume that the tempering process as a diffusion-controlled process which can be described by the Avrami equation. This assumption is not material specific. The value m can be determined using tempering tests by measuring hardness (HV) at different tempering times to obtain different tempering ratio (ι_v) values. Using different tempering ratios and times, values for m and D are obtained by regression analysis.

Substitution of the Equation (38) for the tempering ratio (T_u) into the Johnson-Mehl-Avrami equation (Equation 39) yields (Zhang *et al.*, 2004):

$$H_V = H_\infty + (H_o - H_\infty)Exp[-(Dt)^m]. \tag{41}$$

The values for *m* and *D* are determined for measured hardness data computed from commercially available 'equation solver' software and for the 55NiCrMoV7 (AISI L6) steel were found to equal: $D_o = 2.7 \times 10^8 s^{-1}$, $m = 0.0518$, and $Q = 231$ kJmol^{-1}. This value for Q (activation energy) is consistent with values reported in literature for low and medium alloy steels and is also consistent with expected values for the diffusion of Cr, Mn, Ni, V alloying elements in ferrite (Zhang *et al.*, 2004).

For more complex tempering processes, *e.g.*, double tempering, the following differential equation for the kinetic law of the tempering process must be used to derive values for m and D (Zhang *et al.*, 2004):

$$\tau_V^{\bullet} = (1-\tau_V)mD\left(\ln\frac{1}{1-\tau_V}\right)^{m-1/m} \tag{42}$$

where if $t = 0$, $\iota_V = 0$; the $\dot{\tau}_\upsilon \to \infty$, and if $\iota_V = 1$, $t \to \infty$, then $\dot{\tau}_\upsilon \to 0$.

Figure 24 Illustration of the change in the tempering ratio with respect to time for temperatures between 350°C and 600°C

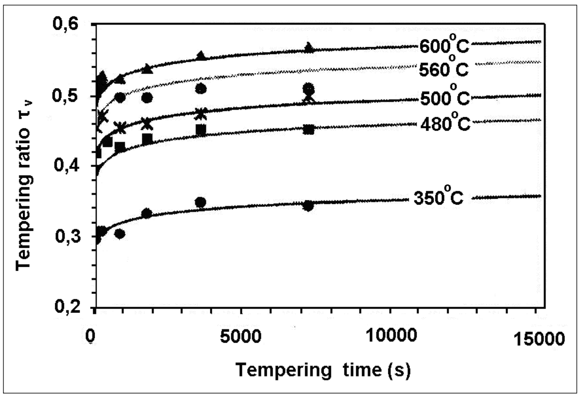

Source: Zhang *et al.* (2004)

This kinetic law provides a relationship between hardness, time and tempering temperature. Figure 24 shows the change of the tempering ratio with respect to time.

Zhang showed that the kinetic law of tempering, which is based on solid state diffusion, Equation (42), can be used for all types of hardness determinations with respect to temperature and time for martensitic steels (Zhang *et al.*, 2004).

2.8 Use of artificial neural networks

Computational Artificial Neural Networks (ANNs) have been used to model a wide range of industrial processes including welding (Stich *et al.*, 1999–2000), cutting tool wear (Stich *et al.*, 1999–2000), effect of tempering on intergranular corrosion of AISI 304L stainless steel (Iacoviello *et al.*, 2003), induction hardening including self-tempering processes (Stich *et al.*, 1999–2000), Jominy curve development (Filetin *et al.*, 1998), mechanical and physical properties of steel (Žmak and Filetin, 1998) and prediction of tempering curve (Žmak and Filetin, 1998; Filetin *et al.*, 1999).

ANNs are computational models that contain many independent simpler computational steps (units) that are designed to be 'trained' and the resulting 'learning' occurs by modifying the weights between the connections which are continually varied computationally until the neural network successfully predicts the desired output values with an acceptable error level (Stich *et al.*, 1999–2000). The components of an ANN are: 'neurons', weights, and learning rules. In general, ANNs are used to determine correlations between input data and a set of output data.

After the neural network training process is completed, a model is developed to provide a correlation between the input and output data. The advantage of ANNs is that they may be used to examine complex processes with many variables, even if the interrelationships between them are not fully understood. Traditionally, linear regression analysis has been used to model such processes, however this approach often fails or provides a poor fit of the data because the interrelationships are non-linear. This is as notable advantage of ANNs for process modelling.

Filetin *et al.* have studied the use of ANNs to model the steel tempering process (Žmak and Filetin, 1998; Reti *et al.*, 1987). Tempering resistance of steels can be characterised by the shape of tempering curves as shown in Figure 25 (Filetin *et al.*, 1999). The shape of the tempering curve depends on the presence and concentration of carbide forming elements: Cr, Mo, W, V, Co.

In the Filetin *et al.* study two steels were studied. One steel designated as: X 40 CrMoV 51 (equivalent to AISI H 13) is a hot working tool steel. The other steel that was modelled was 57 NiCrMoV 77 which has no direct AISI equivalent grade but is reported to be a cold-working tool steel. A total of 18 different alloy chemistries of the two steels were used to develop the model although it was noted that this is a relatively small data set for training and mode or development. After the model was developed, at the conclusion of the training process, eight different steel chemistries of each steel type was used to validate the model. The results obtained are illustrated in Figure 26 (Guo, 1999). Although a good fit was obtained between experimental and modelled data, the models can undoubtedly be improved with the use of a much larger data set.

Figure 25 Examples of tempering curve types: Class 1 represents a carbon or low alloy tool steel, Class 2 represents a medium to high alloy cold-work die steel where carbide precipitation and softening have been inhibited by the ally additions, Class 3 is the curve for a richly alloyed high-speed tool with secondary hardening and Class 4 represents a medium to high alloy hot-die steel with a secondary hardening reaction with relatively low as-quenched hardness

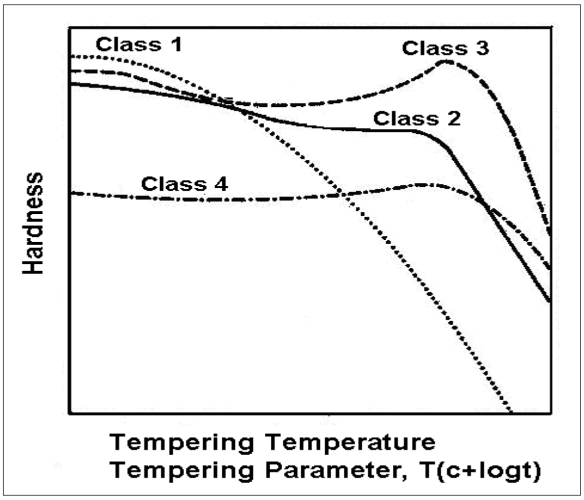

Source: Filetin *et al.* (1999)

Figure 26 Comparison between tempering curves predicted using a neural network model and measured experimental curves for a hot-work and a cold-work tool steel after tempering

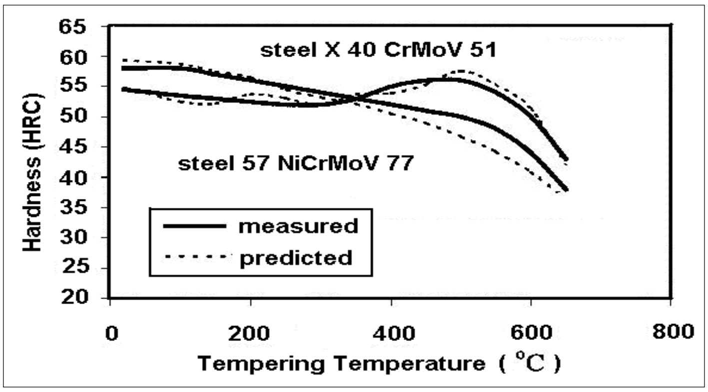

Source: Žmak and Filetin (1998)

2.9 Generalised version of Holloman-Jaffe equation (tempering at variable temperatures)

In some cases, it is necessary to predict the tempering effect that may occur under variable temperature conditions such as the amount of tempering that may occur during heat-up in a tempering furnace. This can be determined from the so-called Generalised Holloman-Jaffe Equation as derived by Reti (Reti *et al.*, 1987; Szilvassy *et al.*, 1994):

$$P_{g,H} = \ln \int_0^t T \exp[CT] t^{T-1} dt. \tag{43}$$

The tempering temperature is constant (T_C), then $T = T_C$ and the well-known Holloman-Jaffe equation is derived (Johnson and Mehl, 1939):

$$P_H = T_C (C + \ln t). \tag{44}$$

Equation (44) can be applied to a case where the temperature is continually changing such as during heat-up in a furnace prior to soaking at temperature. Szilvassy *et al.* derived the following equation for Vickers hardness (HV) for a 0.6% carbon steel during tempering at variable temperature:

$$H(inHV) = 849 - 139.24x \left[\int_0^t T \exp(33.21T) t^{\tau-1} dt \right]^{4.48x10^{-5}} . \tag{45}$$

2.10 Reti's generalised tempering chart

Reti *et al.* (1987) also derived a *generalised* nomogram which may be used to determine the hardness decrease during both isothermal and non-isothermal tempering. The nomogram which is shown in Figure 27 was derived based on the generalised Dorn parameter (P_a) (Reti *et al.*, 1987; Sherby *et al.*, 1957; Orr *et al.*, 1954):

$$P_a = \int_0^t \exp\left[\frac{-Q}{RT}\right] dt \tag{46}$$

where:

Q = activation energy of the process (in kJ mol^{-1} and is alloy chemistry dependent
R = ideal gas constant 8.31 $JK^{-1}mole^{-1}$
T = absolute temperature (K).

Reti also reported the use of a generalised kinetic function to determine hardness resulting from tempering (Reti *et al.*, 1987):

$$H_V = H_{V0} - B \left(\int_0^t \exp\left[\frac{-Q}{RT}\right] dt \right)^n \tag{47}$$

where:

H_V = the hardness estimated at changing tempering temperature
Q = the activation energy for the material
H_{V0} = the hardness of martensite after quenching
B and n = steel composition-dependent constants.

Reti reported that constants Q, B and n can be determined using regression analysis. This is done by first measuring the Vickers hardness of completely martensitic as-quenched steel samples, which is H_{V0}. Tempering tests are then performed using hardness data for a 50CV2 steel (0.5% C, 1.0% Mn, 1.01% Cr, and 0.15% V), of the quenched samples at different tempering temperature and time, and then measuring Vickers hardness (H_V) of the tempered samples. In Equation (45), H_V, H_{V0}, R, T and t are known, and B, Q, n are unknown. The unknowns can be determined when no less than three tempering data points are given. Regression analysis is then used to determine the optimal B, Q and n constants even if more than three tempering data are given. Such calculations were performed using experimentally measured hardness data for 50CV2 steel and values for B, Q and n were calculated regression analysis and found to be 1273, 250 kJ mol^{-1}, and 0.0416 respectively. The as-quenched hardness of the alloy (H_{V0}) was measured to be 780 HV_{10} (Reti *et al.*, 1987).

Figure 27 Reti's Generalised Tempering Chart. The lower part of the nomogram generally interrelates to isothermal tempering processes conducted at different tempering times and temperatures. The upper portion of the nomogram, developed for 50CV2 steel, interrelates the tempering parameter P_a and the as-tempered hardness

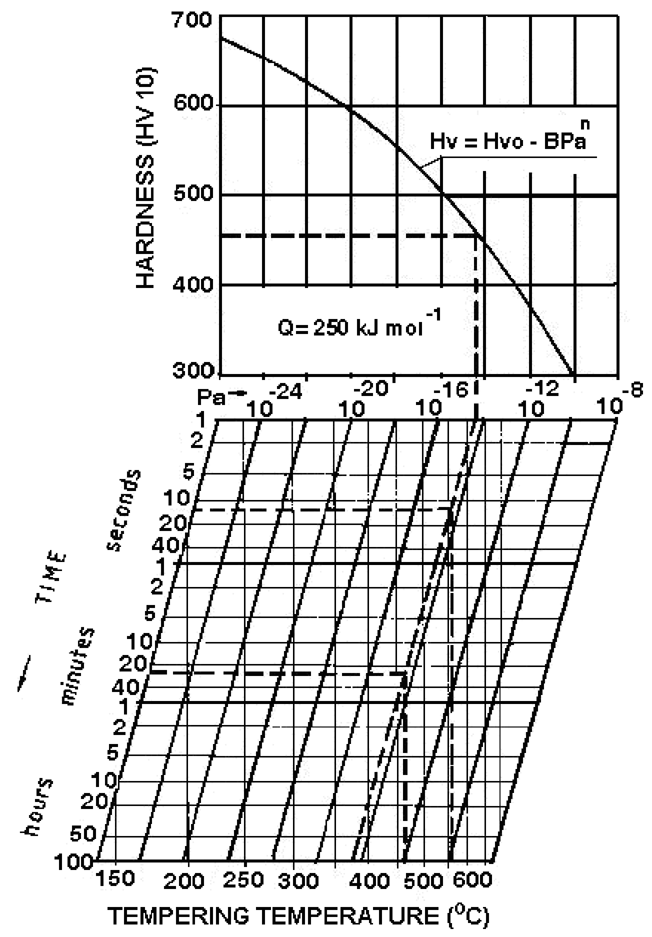

Source: Reti *et al.* (1987)

By substitution of the Dorn parameter into the generalised kinetic function (Equation 47), the following equation was derived (Reti *et al.*, 1987):

$$H_V = H_{V0} - BP_a^n. \tag{48}$$

This equation was used to develop the nomogram shown in Figure 27 which is characterised by two parts (Reti *et al.*, 1987). The lower portion of Figure 27 is characterised by an isothermal process and interrelates the tempering parameter (P_a) to tempering temperature and time. This part of the chart can be used to determine the any temperature or time if any other temperature-time combination are known (to achieve the same hardness value).

The upper portion of Figure 27 was developed based on AFNOR NF 50CV2 steel (0.5% C, 1.0% Mn, 1.01% Cr, 0.15% V) and interrelates the tempering parameter and hardness and while the lower portion of the chart may be used for any steel (not containing Mo), the upper portion must be developed for each steel alloy of interest. For non-isothermal processes, the value of P_a to achieve the desired hardness may be determined using the upper portion of Figure 27 and the various time-temperature combinations to achieve that hardness is then determined from the lower portion of the nomogram.

2.11 Liu equation and nomogram for equivalent tempering of steel (alloy 40CrNiMoA)

Liu (1985) reported that generally the precision of the tempering condition predictions for may steels is insufficient to allow general use. This is primary because the Holloman-Jaffe equation does not account for the variability of both temperature and time in the overall hardness prediction. To obtain a significant improvement in the precision of the tempering parameter prediction, a multiple linear regression equation was developed. While the equation that was developed was for the steel alloy 40CrNiMoA (AISI 4340), the approach reported could be utilised for other steel grades if appropriate experimental work were performed.

The first step in this process was to machine 10 mm × 10 mm × 5 mm steel test specimens. They were then austenitised at 860°C (T_A) and oil quenched to a Rockwell hardness of 50–55. Three test specimens (triplicate analysis) were then tempered at predetermined temperatures and times (see Table 4) and the hardness was measured and the data for the three test specimens was averaged.

Table 4 Tempering data obtained for experimental 40CrNiMoA test specimens (average of triplicate analysis)

Tempering temperature (°C)	*HRC at tempering time (h)*							
	0.08	*0.15*	*0.50*	*1*	*2*	*3*	*5*	*10*
200	51.0	50.8	50.5	50.4	50.2	50.1	49.8	49.6
300	48.9	48.6	48.0	47.7	47.2	46.9	46.6	46.0
400	46.5	45.5	44.8	44.0	43.5	43.0	42.5	42.0
500	43.0	41.2	40.0	38.9	37.5	37.0	36.5	36.0
600	38.5	38.0	33.5	32.0	30.5	28.8	27.0	26.5

Using the data from Table 4, which is shown graphically in Figure 28, it was then possible to generate an equivalent tempering nomogram for the 40CrNiMoA steel alloy which is shown in Figure 29 (Liu, 1985).

Figure 28 Correlation of as-tempered hardness with tempering temperature for 40CrNiMoA (AISI 4340) steel alloy

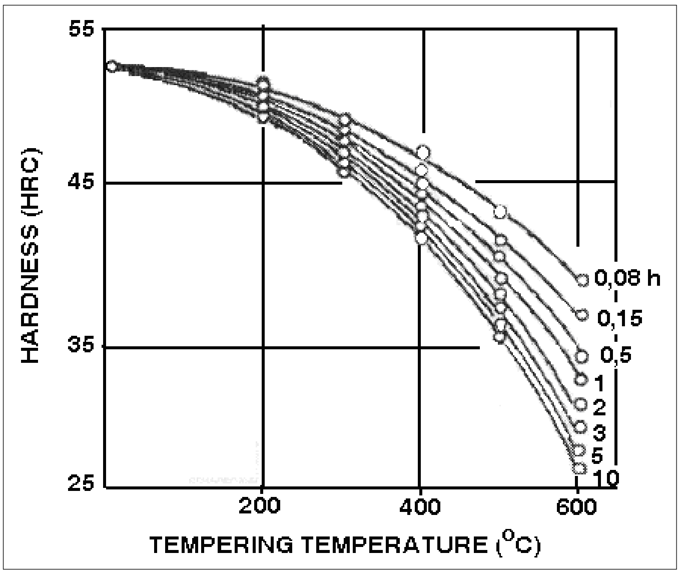

Source: Liu (1985)

Figure 29 Liu's equivalent tempering nomogram for 40CrNoMoA (AISI 4340 steel) where tau (ι) is the isothermal tempering time in hours, p is the tempering parameter, HRC is the as-tempered Rockwell C hardness of the 40CrNoMoA steel, and °C is the tempering temperature

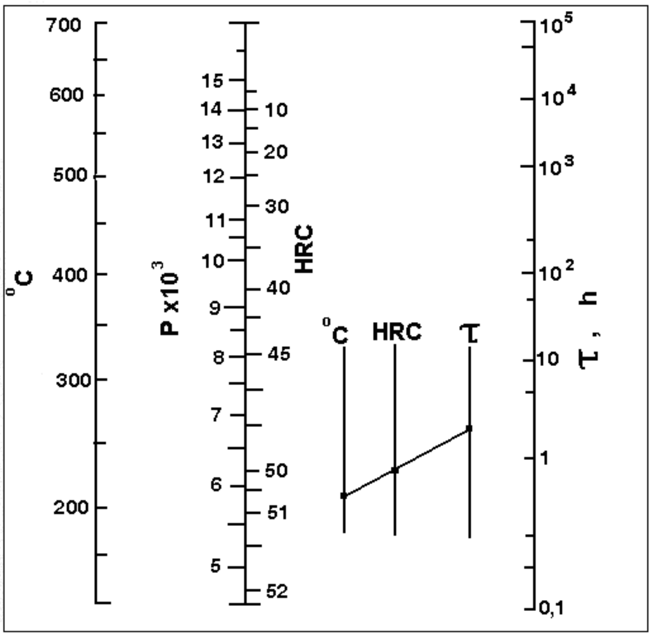

Source: Liu (1985)

This nomogram interrelates steel hardness, tempering time and temperature. Using this nomogram (which is only good for the alloy for which it was determined, in this case 40CrNiMoA (Chinese standard steel is: 0.37%–0.44% C, 0.60%–0.90% Cr, 1.25%–1.65% Ni, 0.15%–0.25% Mo, 0.17%–0.37% Si, 0.50%–0.80% Mn, <0.030% P, <0.030% S), which is also nominally equivalent to AISI E4340H, it is possible to determine the tempering temperature if the desired hardness and time are known, tempering time if the desired hardness and temperature are known or the as-tempered hardness for any combination of tempering temperature-time combinations.

(Note: The 'A' designation in the steel grade 40CrNiMoA refers to the quality class of the steel. Besides 40CrNiMoA, there is: 40CrNiMoB, 40CrNiMoC or 40CrNiMoD. Here 'A', 'B', 'C' and 'D' are all class types. However, for the work performed by Liu, 40CrNiMoA steel was used.)

Multiple linear regression analysis was performed on the data shown in Table 4. The final form of the regression equation which as used to predict as-tempered hardness for 40CrNoMoA steel that was obtained after analysis was:

$$52.5 - HRC = \left(1.087 \times 10^{20}\, t e^{-36.132/RT}\right)^{0.12} \tag{49}$$

where:

52.5 = as-quenched hardness for the alloy 40 CrNiMoA
HRC = as-tempered hardness targeted
ι = tempering time (hours)
36.132 = activation energy (Q) for the tempering process (cal mole^{-1})
T = tempering temperature (K)
R = ideal gas constant (8.31 JK^{-1}mole^{-1}).

Liu found this regression equation which was developed from the experimental data shown in Table 4 and exhibits a correlation of R = 0.9984 provided a much better fit with less error with respect to tempering time and temperature than did the Holloman-Jaffe equation of the form: P = T(c + log t). However, this analysis must be developed for each alloy of interest.

2.12 Limitations of tempering parameters

In spite of the development work reported thus far relating to the use of tempering parameters to predict properties such as steel hardness, strength, ductility, and notch toughness a number of limitations have been identified. Enami *et al.* (1974) studied the effect of cooling rates and tempering conditions on the use of Mn-Ni-Mo (0.20% C, 0.29% Si, 1.37% Mn, 0.68% Ni, 0.01% Cr, 0.58% Mo, 0.036% Al, 0.012% P, 0.007% S) and Cr-Mo (0.13% C, 0.24% Si, 0.60% Mn, 0.03% Ni, 2.40% Cr, 0.92% Mo, 0.001% Al, 0.012% P, 0.010% S) steels for pressure vessels (see Figure 30). They found that the strength continuously decreased as the tempering parameter P = T(20 + log t) increased; although the ductility and the toughness did gradually improve and then passed through a maximum value, and then decreased. The magnitude of this effect was dependent on both cooling rates and tempering conditions. Generally, the tempering parameter corresponding to maximum toughness was dependent on the cooling rates for Mn-Ni-Mo steel, but not for Cr-Mo steel. However, the maximum toughness for both steels was dependent on cooling rates. Ductility effects for both steels, as predicted by the tempering parameter, were not dependent on cooling rates (Enami *et al.*, 1974).

In a recent US Department of Energy Study, it was reported that although various models have been developed to predict as-tempered hardness of steels as a function of wrought steel composition, initial microstructure, tempering time and tempering temperature, in some cases, they were not applicable to for use in steel foundries (Aichbhaumik *et al.*, 2004). This is because specific heat-up and soaking times are often specified in national and international standards and that these times are often considerably longer, due to mass and furnace loading effects than conditions predicted by the models reported to date. However, it was acknowledged that these models may have utility to estimate heat treatment and steel composition control necessary to obtain a specific final as-tempered hardness (Aichbhaumik *et al.*, 2004).

One of the greatest limitations to many of the models reported to date is that they do not account for the significant tempering effects that will occur as the load heats up in the furnace to the final soaking temperature. In addition, these results will be affected by furnace loading, and section size of the parts (Aichbhaumik *et al.*, 2004).

Figure 30 Effects of cooling rate and Holloman-Jaffe tempering parameter on Vicker's hardness of Mn-Ni-Mo and Cr-Mo steels

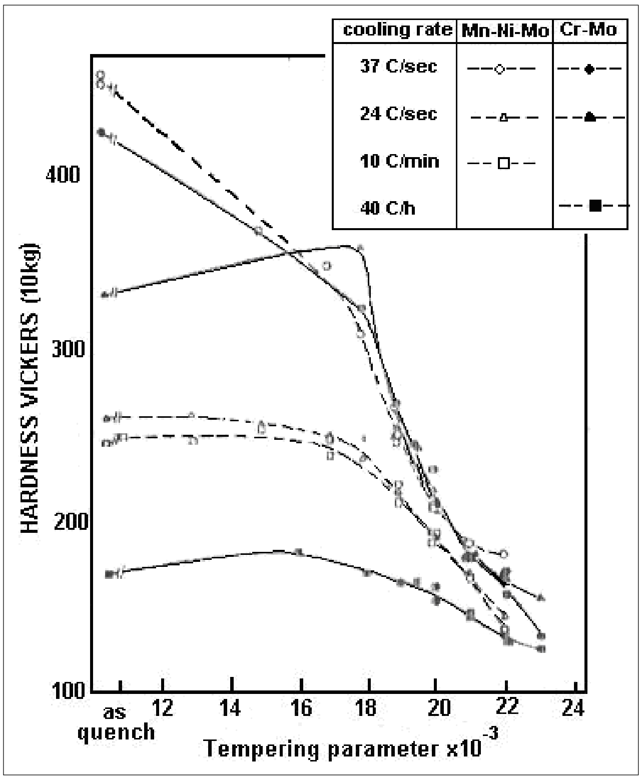

Source: Enami *et al.* (1974)

One approach that has been developed to address the combined effects of both temperature and time during heating-up of the load and subsequent soaking is the use of a normalised 'extent of tempering parameter' (E) shown by Equation (39) (Aichbhaumik *et al.*, 2004). The 'extent of tempering parameter' (E), which has been extensively evaluated in various casting foundries, was found to be much more affected by varying tempering temperature than tempering time. The principle limitation of this parameter is that although it does provide insight into variations occurring in a tempering furnace, it cannot be use to estimate as-tempered hardness. (The constants used for performing calculations with Equation (39) are provided in Table 5 (Aichbhaumik *et al.*, 2004) (Interestingly, the activation energies reported by Aichbhaumik *et al.* in Table 5 are considerably lower than those reported by other authors cited in this review.)

$$E = \frac{0.3\sqrt{D_0 t_{ramp,load} e^{-Q/RT_1}} + \sqrt{D_0 t_{hold,load} e^{-Q/RT_1}}}{0.3\sqrt{D_0 t_{ramp,controller} e^{-Q/RT_1}} + \sqrt{D_0 t_{hold,controller} e^{-Q/RT_2}}} \tag{50}$$

where:

T_1 = 95% of the difference between steady state temperature and room temperature
T_2 = set-point temperature
$t_{ramp,load}$ = time in seconds for the load to reach T_1
$t_{hold,load}$ = time in seconds for the load to reach or exceed T_1
$t_{ramp,controller}$ = time in seconds for controller to reach T_1
$t_{hold,controller}$ = time in seconds for controller to reach or exceed the set-point temperature
D_o = diffusion coefficient (see Table 5)
Q = activation energy (see Table 5)
T = the temperature in Kelvin.

Table 5 Diffusion constants for calculation of extent of tempering parameter

Steel alloy	*Thermal process*	*Lattice type*	*Valid temperature °C (°F)*	*Diffusion coefficient D_o (cm^2/s)*	*Activation energy – Q kJ/mole (kcal/mole)*
Low and medium alloy steels	Tempering	BCC	723 (<1333)	0.02	100.9 (24.1)
Low and medium alloy steels	Austenitising	FCC	723 (>1333)	0.12	133.9 (32.0)
High alloy steels	Solutionising	FCC	–18 (>0)	0.32	158.3 (37.8)

Notes: Diffusion coefficient at 298K.
Activation energy.

2.13 Inoue's lambda value

Inoue (1980) has developed a so-called lambda (λ) value, which is a 'heating parameter', to address the problem of the degree of tempering that occurs during heat-up as well as when the steel is at the desired soaking temperature. An illustration of a typical tempering curve is shown in Figure 31 (Just, 1976).

Figure 31 Illustration of a typical tempering curve with time steps used to calculate a heating cycle

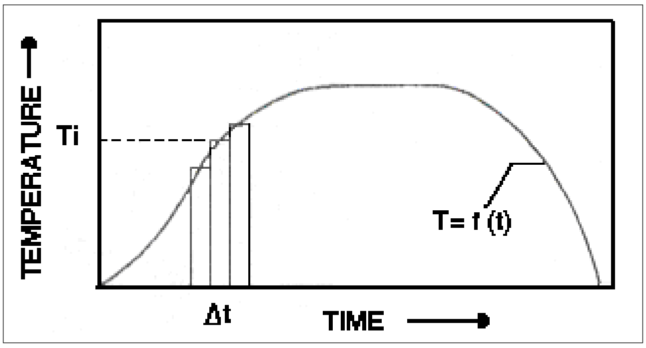

Source: Just (1976)

The lambda-value (λ) is used to compute the relative effects of heating time and temperature. It is derived from (Inoue, 1982):

$$C = r.t = A.t.\exp\left(\frac{-Q}{RT}\right) \tag{51}$$

$$\log C = \log A + \log t - \frac{Q}{2.3R} \times \frac{1}{T} \tag{52}$$

where:

log A = where (A) is a pre-exponential factor for the Arrhenius equation and is assumed to be 50 for most steels

t = tempering time (min)

Q = activation energy for the tempering process which were reported to be 70 kcal/mol (295 kJ/mole) for plain carbon steel, and approximately 100 kcal/mole (420 kJ/mole) for a Cr-Mo steel and which increases with alloying element content (Inoue, 1980)

R = ideal gas constant (8.31 $\mathrm{JK^{-1}mole^{-1}}$)

T = tempering temperature (K).

The λ-value is used to represent log C and using these assumptions, a more practical expression is derived:

$$\lambda = \log t - \frac{Q}{4.6} \times \frac{1}{T} + 50. \tag{53}$$

Determination of various tempering time or temperatures is determined from the following equation, if one set of time and temperature conditions is known (Inoue, 1982):

$$\frac{t_1}{t_2} = \exp\left[\frac{Q}{1{,}987}\left(\frac{1}{T_2} - \frac{1}{T_1}\right)\right]. \tag{54}$$

It is known that alloying elements exhibit a strong effect on the activation energy (Q). Mn and Mo exhibit a strong influence and Cr exhibits a comparatively lower influence. To address this potential problem, a correction of the activation energy ($Q_{\text{corrected}}$) is made as follows (Inoue, 1982):

$$\%Mo_{eq} = \%Mo = 1/5\%Mn + 1/10\%Cr \tag{55}$$

$$Q_{corrected} = 114.7 \times \%Mo_{eq} + 46.6. \tag{56}$$

Once a λ-value is calculated for a set of temperature and time conditions of interest, it is possible to calculate mechanical properties such as tensile strength or yield strength for any combination of temperature and time conditions within the range of 400°C–700°C using Table 6 (Inoue, 1980; 1982).

Table 6 Inoue's lambda value, temperature, tensile strength and yield strength correlation

Tempering temperature (°C)	*Lambda value*	*Tensile strength kgf/mm²*	*Yield strength kgf/mm²*
400	18.2	154	148
450	20.4	139	133
500	22.3	120	114
550	24.0	113	106
575	24.7	107	98
600	25.5	104	97
625	26.1	101	88
650	26.8	92	83

These equations are used as follows:

- Use Equation (53) to calculate the desired lambda value for a given set of tempering temperature and time conditions.
- Use Equation (54) to calculate tempering temperature or time if a given set of conditions are known in order to obtain equivalent tempering results.
- The lambda values for a heating cycle may be calculated using the concept of a time step illustrated in Figure 31. In this case, using Equation (53), an incremental λ-value ($\Delta\lambda_i$), for i time steps, is calculated. An average temperature for each time step is used for the calculation. The $\Delta\lambda_i$ are summed over all time steps from the beginning to the end of the tempering process, including the heat-up and soaking time, to achieve a final total λ-value using the following equation:

$$\lambda = \log(10^{\Delta\lambda i} + 10^{\Delta\lambda i+1} + 10^{\Delta\lambda i+2} + \ldots\ldots. \tag{57}$$

This general approach was used by Inoue (1980) to determine as-tempered mechanical properties for S 40C (AISI 1040), SMn 443 (AISI 1541), SCr 440 (AISI 5140), and SCM 440 (AISI 4140) steels.

2.14 Pont P *parameter*

Pont *et al.* (1967) have also developed a tempering parameter (P) based on the activation energies of diffusion:

$$P = \left(\frac{1}{T} - \frac{nR}{\Delta G} \times \log \frac{t}{t_0} \right)^{-1} \tag{58}$$

where:

ΔG = activation energy for tempering (57.5 Kcal/mol). This value is independent of the carbon content of the steel and it is representative of the activation energy for self-diffusion of alpha iron
T = tempering temperature (K)
t = tempering time
t_0 = reference time
R = gas constant (8.31 $\mathrm{JK^{-1}mole^{-1}}$)
$n = \log_{10}$.

Pont *et al.* (1967) then derived the expression for Vicker's hardness (H_V):

$$H_V = f\left(\frac{1}{P} \right) = f\left(\frac{1}{T} - \frac{nR}{\Delta G} \times \log \frac{t}{t_0} \right)^{-1}. \tag{59}$$

Using different carbon content steels since 0,1%, Pont and co-authors performed tempering studies using constant parameter (Hollomon and Jaffe, 1945; Grange and Baughman, 1956; Pont *et al.*, 1967). Figures 32(a) and 32(b) show these results.

Figure 32 Tempering results from constant parameter for temperatures: (a) 400°C, 500°C, 600°C, 700°C and (b) 450°C, 550°C, 650°C, 750°C

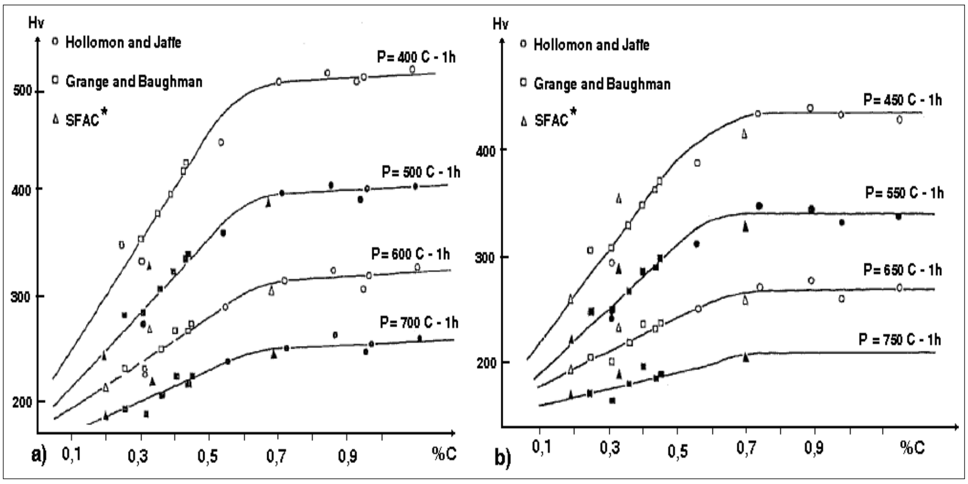

Notes: * *S*ociete des *F*orges et *A*teliers du *C*reusot. Chemistries are provided in Table 7.

Source: Pont *et al.* (1967)

Using values obtained from Figures 32(a) and 32(b), Pont parameter nomogram was built (Figure 33). In this illustration converging Vickers hardness curves with varying tempering temperatures and Pont parameters (P) for a steels with different carbon contents are shown (Pont *et al.*, 1967).

Figure 33 Tempering curves for initial martensitic microstructure from different carbon contents

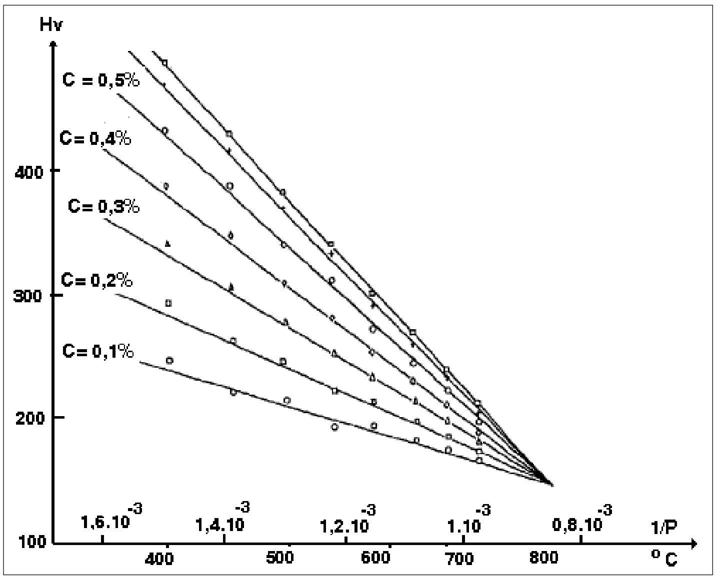

Note: Chemistries are provided in Table 7.

Source: Pont *et al.* (1967)

Steel compositions used in theses studies are shown in Table 7.

Table 7 Steel compositions used in the Figures 32(a), 32(b) and 33

Steel designation	*C*	*Mn*	*Si*	*S*	*P*	*Ni*	*Cr*	*Cu*	*Al*	$Hv_{initial}$
Hollomon and Jaffe										
U	0.31	0.52	0.10	0.026	0.07		0.015	0.06		476
S	0.56	0.54	0.18	0.015	0,012		0.02			786
T	0.74	0.66	0.18	0.021	0,009		0.01			890
W	0.89	0.55	0.06	0.020	0,012		0.01	0.08		900
R	0.98	0.30	0.30	0.021	0,007		0.03	0.055		890
V	1.15	0.58	0.09	0.021	0,012		0.01			826
Grange and Baughman										
1026	0.25	0.79	0.11	0.026	0.012	0.02				
1030	0.31	0.57	0.09	0.025	0.008	0.02	0.02			
1035	0.36	0.74	0.24	0.030	0.019	0.02	0.07		0.01	
1040	0.40	0.60	0.27	0.013	0.010	0.02	0.02		0.01	
1042	0.44	0.79	0.24	0.030	0.020	0.01	0.02		0.01	
1045	0.45	0.73	0.17	0.030	0.017	0.13	0.02		0.01	

Table 7 Steel compositions used in the Figures 32(a), 32(b) and 33 (continued)

Steel designation	*C*	*Mn*	*Si*	*S*	*P*	*Ni*	*Cr*	*Cu*	*Al*	$Hv_{initial}$
S.F.A.C.										
A9/10	0.09	0.60	0.18	0.029	0.029	0.13	0.095	0.06	0.035	176
										160
										147
A9	0.19	0.51	0.22	0.023	0,025	0.23	0.14		0.04	384
										199
										163
A6	0.33	0.485	0.345	0.038	0,019	0.155	0.12		0.015	530
										366
										193
AOV	0.70	0.63	0.17	0.012	0,013	0.04	0.02	0.08	0.01	858
										399
										316
										226

Note: Elements in % weight.

Source: Pont *et al.* (1967)

3 Conclusion

Although the Holloman-Jaffe (Larsen-Miller) tempering parameter equations continue to be used in the heat treatment industry, a number of shortcomings have been identified including problems of their precision in prediction of hardness as a result of tempering but most importantly, these expressions do not address non-isothermal tempering conditions. In this paper, various methods of addressing these deficiencies have been briefly reviewed, all of which represent potentially significant advantages over the now-classical Holloman-Jaffe equation.

Acknowledgements

Sincere appreciation to Mr. Kyozo Arimoto for his vital assistance in identifying a number of the tempering parameters reported herein and for his patience and assistance in translating a number of the supporting documents cited.

References

Aichbhaumik, D., Blair, M., Wong, H., Charles, M., Deskevich, N., Varkey, V., Voigt, R. and Wollenberg, A. (Project Team) (2004) Heat Treatment Procedure Qualification: Final Technical Report, U.S. Department of Energy Contract No. DE-FC07-99ID13841.

Andrews, K.W. (1959) 'Some observations on the use of a time-temperature parameter', Special Report No. 64, The Iron and Steel Institute, pp.292–294.

Anonymous (1985a) 'Techcommentary – induction heat treatment', Newsletter published by EPRI Center for Materials Fabrication, EMF, Columbus, Ohio, Vol. 2, No. 2.

Anonymous (1985b) 'Techcommentary – induction tempering', Newsletter published by EPRI Center for Materials Fabrication, EMF, Columbus, Ohio, Vol. 2, No. 4.

Avrami, M. (1939) 'Kinetics of phase change – general theory', *J. Chem. Phys.*, Vol. 7, No. 12, pp.1103–1112.

Avrami, M. (1940) 'Kinetics of phase change. II transformation-time relations for random distribution of nuclei', *J. Chem. Phys.*, Vol. 8, No. 2, pp.212–224.

Avrami, M. (1941) 'Granulation, phase change, and microstructure kinetics of phase change. III', *J. Chem. Phys.*, Vol. 9, No. 2, pp.177–184.

Brown, W.F., Succop, G. and Manson, S.S. (1954) 'Written discussion', *Transaction of ASM*, Vol. 46, Part 2, pp.1400–1404.

Davis, J.R. (Ed.) *ASM Materials Engineering Dictionary*, ASM International, Materials Park, Ohio.

DiMelfi, R.J. (1978) 'Comments on understanding the Larsen-Miller parameter – in F.T. Furillo, S. Purushothaman, and J.K. Tien', *Scripta Metallurgica*, Vol. 12, pp.327–329.

Enami, T., Sato, S., Tanaka, T. and Funakoshi, T. (1974) 'Effects of cooling rates and tempering conditions on the strength and toughness of Mn-Ni-Mo, Cr-Mo steel plates', *Kawasaki Steel Giho*, Vol. 6, No. 2, pp.145–161.

Engel, E.H. (1939) 'The softening rate of a steel when tempered from different initial structures', *Trans. Am. Soc. Met.*, Vol. 27, pp.1–15.

Filetin, T., Majetić, D. and Žmak, I. (1998) 'Application of neural network for prediction the Jominy curves', *Proceedings of the 11th Congress of the Int. Federation for Heat Treatment and Surface Engineering and 4th ASM Heat Treatment and Surface Eng. Conference in Europe*, Florence, Vol. III, pp.353–361.

Filetin, T., Majetić, D. and Žmak, I. (1999) 'Predicting the tempering curve of tool steels using neural networks', *Proceedings of the 2nd International Conference on Industrial Tools*, ICIT, Maribor, Slovenia, pp.424–427.

Fullman, R.L. (1954) 'Written discussion', *Transactions of ASM*, Part 2, Vol. 46, pp.1398–1400.

Furillo, F.T., Purushothaman, S. and Tien, J.K. (1978) 'Further discussion on understanding the Larsen-Miller parameter', *Scripta Metallurgica*, Vol. 12, pp.331–332.

Gingras, R. and Grenier, M. (2005) 'Software assists in optimizing tempering process', *Industrial Heating*, December, Vol. 72, No. 12, pp.49–52.

Grange, R.A. and Baughman, R.W. (1956) 'Hardness of tempered martensite in carbon and low alloy steels', *Transactions of American Society for Metals*, Vol. XLVIII, pp.165–197.

Grange, R.A., Hribal, C.R. and Porter, L.F. (1977) 'Hardness of tempered martensite in carbon and low-alloy steels', *Metallurgical Transactions A*, Vol. 8A, November, pp.1775–1785.

Gulvin, T.F., Scott, D., Haddrill, D.M. and Glen, J. (1972–1973) 'Paper no. 621 – the influence of stress relief on the properties of C and C-Mn pressure-vessel plate steels', *J. of West of Scotland Iron and Steel Institute*, Vol. 80, pp.149–175.

Guo, C. (1999) 'Mathematical model for tempering time effect on quenched steel based on Hollomon parameter', *Acta Metall. Sin.*, Vol. 35, No. 8, pp.865–868.

Hollomon, J.H. and Jaffe, J.H. (1945) 'Time-temperatures relations in tempering steel', *Transactions of the American Institute of Mining and Metallurgical Engineers*, Vol. 162, pp.223–249.

Huang, R. (2003) *ASE324: Aerospace Materials Laboratory – Lecture 10*, Department of Aerospace Engineering and Engineering Mechanics, The University of Texas at Austin, 30 September.

Iacoviello, D., Iacoviello, F. and Macario, M. (2003) 'Neural networks application in an AISI 304L intergranular corrosion resistance analysis', *MED03 – The 11th Mediterranean Conference on Control and Automation*, Paper No. T3-025, Rhodes, Greece, 18–20 June.

Inoue, T. (1980) 'A new tempering parameter and its application to the integration of the tempering effect of continuous heat cycle', *Tetsu-to-Hagane (Journal of the Iron and Steel Institute of Japan)*, Vol. 66, No. 10, pp.1532–1541.

Inoue, T. (1982) 'A new tempering parameter and its use for practical heat treatment', *Netsu-Shori*, Vol. 22, No. 1, pp.25–29.

Jarl, M., Berntsson, T., Sapcanin, E. and Azizi, B. (2003) 'Replacement of lead baths for the tempering of spring wire', *Scandinavian J. of Metallurgy*, Vol. 32, pp.241–246.

Johnson, W.A. and Mehl, R.F. (1939) 'Reaction kinetics in processes of nucleation and growth', *Trans. AIME*, Vol. 135, No. 8, pp.396–415.

Jost, S., Langer, H., Pietsch, D. and Uhlig, P. (1976) 'Rechnerische Ermittlung der Erwärmdauer bei der Wärmebehandlung von Stahl', *Fertigungstechnik und Betreib*, Vol. 26, No. 5, pp.298–301.

Just, E. (1976) 'Vergüten. Werkstoffbeeinflussung durch Härten und Anlassen', *VDI Berichte*, No. 256, pp.125–140.

Kern, R.F. and Suess, M.E. (1979) 'Chapter 6 – hardenability and tempering parameter', *Steel Selection: A Guide for Improving Performance and Profits*, New York, NY: J. Wiley and Sons, pp.82–113.

Krauss, G. (1980) 'Chapter 8 – tempering of steel', *Principles of Heat Treatment of Steel*, American Society for Metals, Metals Park, Ohio, pp.187–227.

Larson, F.R. and Miller, J. (1952) 'A time-temperature relationship for rupture and creep stresses', *Trans. for the American Society of Mechanical Engineers*, Vol. 74, pp.765–775.

Liscic, B. and Filetin, T. (1987) 'Computer-aided determination of the process parameters for hardening and tempering structural steels', *Heat Treatment of Metals*, Vol. 3, pp.62–66.

Liu, G. (1985) 'A nomograph and equation of equivalent tempering for steel 40CrNiMoA', *Iron and Steel*, Vol. 20, No. 7, pp.21–26.

Manning, C.R. (1960) 'Application of rate-temperature parameters to tensile data for magnesium allows and a relation between the Larson-Miller constant and the activation energy', NASA Technical Note D-172, May.

Manson, S.S. and Brown, W.F. (1952) 'Time – temperature stress relations for the correlation and extrapolation of stress-rupture data', *Transaction of ASME*, Vol. 74, pp.765–775.

Manson, S.S. and Haferd, A. (1953) *A Linear Time-Temperature Relation for Extrapolation of Creep and Stress-Rupture Data*, National Advisory Committee for Aeronautics (NACA), T.N. 2890, March.

Mendelson, A., Roberts, E. and Manson, S.S. (1965) 'Optimization of time-temperature parameters for creep and stress rupture with application to data from German cooperative long-time creep program', NASA Technical Note D-2975, August.

Murphy, S. and Woodhead, J.H. (1972) 'An investigation into the validity of certain tempering parameters', *Metallurgical Transactions*, Vol. 3, March, pp.727–735.

Nehrenberg, A.E. (1950) 'Master curves simplify stainless tempering', *Steel*, 23 October, Vol. 127, pp.72–76.

Orr, R.L., Sherby, O.D. and Dorn, J.E. (1954) *Transactions of ASM*, Vol. 46, pp.113–128.

Pink, E. (1994) 'Physical significance and reliability of Larson-Miller and Manson-Haferd parameters', *Materials Science and Technology*, Vol. 10, pp.340–344.

Pont, G., Maynier, Ph. and Martin, P.F. (1967) 'Application D'Une Équivalence Entre Le Temps Et La Tempèrature A L'étude Du Revenu Des Aciers', *Revue de Métallurgie*, December, pp.1115–1125.

Ramierez, J.E., Mishael, S. and Shockley, R. (2005) 'Properties and sulfide stress cracking resistance of coarse-grained heat-affected zones in V-Microalloyed X60 steel pipe', *Welding Journal*, July, pp.113–123.

Reti, T., Gergely, M. and Tardy, P. (1987) 'Mathematical treatment of non-isothermal transformations', *Materials Science and Technology*, Vol. 3, May, pp.365–372.

Semiatin, S.L., Stutz, D.E. and Bryer, T.G. (1985a) 'Induction tempering of steel: Part I – development of an effective tempering parameter', *Journal of Heat Treating*, Vol. 4, No. 1, pp.39–46.

Semiatin, S.L., Stutz, D.E. and Bryer, T.G. (1985b) 'Induction tempering of steel: Part II – effect of process variables', *Journal of Heat Treating*, Vol. 4, No. 1, pp.47–55.

Sherby, O.D., Lytton, J.L. and Dorn, J.E. (1957) 'Activation energies for creep of high-purity aluminum', *Acta Metallurgica*, Vol. 5, April, pp.219–227.

Sinha, A.K. (2003) 'Chapter 14 – tempering', *Physical Metallurgy Handbook*, New York, NY: McGraw-Hill, pp.1445–1450.

Stich, T.J., Spoerre, J.K. and Velasco, T. (1999–2000) 'The application of artificial neural networks to monitoring and control of an induction hardening process', *J. Industrial Technology*, November–January, Vol. 16, No. 2, pp.2–11.

Szilvassy, C.C., Gergely, M. and Reti, T. (1994) 'Computer simulation of heat treatment transformation processes', *Journal of Metallurgy*, Vol. 232, No. 3, pp.121–127, http://www.macaudata.com/macauweb/book138/html/12601.htm.

Taylor, P.R. and Johnson, R.F. (1971) 'Analysis of long-term creep rupture and elevated-temperature yield or proof-stress data', *Journal of the Iron and Steel Institute*, September, pp.714–720.

Trowsdale, A.J. and Pritchard, S.B. (2006) 'Dual phase steel – high strength fasteners without heat treatment', http://www.corusautomotive.com/file_source/StaticFiles/Microsites/Automotive/Technical/Final_CBM_Dupla_Paper.pdf.

Ulff, C. (1970) 'Effect of stress-relief annealing on the mechanical properties of steel grades for pressure vessels', *Jem-kontorets annaler*, Vol. 154, No. 2, pp.53–64.

Waisman, J.L. and Snyder, W.T. (1949) 'Predicting the effect of complex tempering cycles', *Trans. of the ASM*, Vol. 41, pp.1400–1414.

Wan, N., Xiong, W. and Suo, J. (2005) 'Mathematical model for tempering time effect on quenched steel based on Holloman parameter', *J. Mater. Sci. Technol.*, Vol. 21, No. 6, pp.803–806.

Zhang, Z., Delagnes, D. and Bernhart, G. (2004) 'Microstructure evolution of hot-work tool steels during tempering and definition of a kinetic law based on hardness measurements', *Materials Science and Engineering*, A, Vol. 380, pp.222–230.

Zikeev, V.N., Kornyushchenkova, Yu.V. and Izvil'skii, V.V. (1984) 'Influence of the temperature-time parameter of tempering on the properties of 18Kh1G1MF steel resistant to hydrogen embrittlement', *Metal Science and Heat Treatment*, Vol. 26, Nos. 1–2, pp.99–102.

Žmak, I. and Filetin, T. (1998) 'Neural network in predicting steel properties: artificial neural networks as a tool in predicting mechanical and thermal properties of steels', *Proceedings of the 11th Congress of the International Federation for Heat Treatment and Surface Engineering*, Florence, Italy, pp.353–361.